Accepted manuscript (author version)

To appear in:

Iranian Journal of Earth Sciences (Iran J. Earth. Sci.)

E-ISSN: 2228-785X Print ISSN: 2008-8779

Received: 8 January 2025

Revised: 11 April 2025

Accepted: 27 August 2025

DOI: https://doi.org/10.57647/j.ijes.2025.17557

Original Research

Facies analysis and depositional environment of the Upper Miocene-Pliocene deposits (Aghajari Formation) in the Afrineh syncline, southwest of Lorestan

Mostafa Sedaghatnia[1], Behrouz Rafiei[1*], Bizhan Yousefi Yegane[2]

[1]Department of Geology, Faculty of Sciences, Bu–Ali Sina University, Hamedan, Iran

[2] Department of Geology, Faculty of Sciences, Lorestan University, Khorram Abad, Lorestan

* Corresponding author: b_rafiei@basu.ac.ir

Abstract

The Aghajari Formation is found across the Zagros Folded Zone. The purpose of this research is to investigate the depositional environment of the Aghajari Formation (Upper Miocene-Pliocene) in southwest Lorestan. Seven stratigraphic sections were selected in the Afrineh syncline. The Aghajari Formation, more than 500 meters thick, consists of conglomerate (to a lesser extent), sandstone, siltstone, mudstone, and shale. Field investigations resulted in recognition of eighteen lithofacies, which comprise three conglomerate lithofacies (Gm, Gp, Gt), nine sandstone lithofacies (Sp, St, Sm, Sh, Sr, Sfl, Sl, Slr, Sr (Fl)), four mudstone lithofacies (Fm, Fl, Fcf, Fl(Sr)), a gray shale lithofacies rich in planktonic fauna, and a bioclastic grainstone facies. The Skolithos facies was also identified. In the sandstones, two petrofacies, chertarenite and calclitharenite, were recognized. The lower part of the Aghajari Formation was deposited in a meandering river environment. Along with sea transgression, these deposits were overlain by the tidal flat deposits, and marine facies were deposited at the end of the sequence. The bioclastic grainstone and the gray shale are associated with shallow and deeper marine environments, respectively. The changes in the depositional environment in the lower part of the Aghajari Formation were caused by the sea-level change. Following the deposition of marine shale, due to sea-level fall and regional tectonics, the studied sequences underwent a marine regression, resulting in the formation of fluvial deposits. The depositional environment changes occurred during the Miocene and Pliocene.

Keywords: Lithofacies analysis, Depositional environment, Aghajari Formation, Miocene-Pliocene, Afrineh syncline, Lorestan

1. Introduction

The Aghajari Formation belongs to the Fars Group, officially introduced by James and Wynd (1965). This formation consists of a thick sequence of red siliciclastic sediments, reaching up to 3000 meters in some instances. It extends across extensive regions of Lorestan, Khuzestan, and Fars provinces and even spans into Iraq, Syria, and Turkey (Alavi, 1994; Motiei, 1995; Sakhavati et al., 2020). The type section of the Aghajari Formation, which is 2966 meters thick, has been examined in the Aghajari oil field wells. It is characterized by repeated cyclic patterns that thin out towards the top (Alavi, 2004; Sahraeyan et al., 2012; Motiei, 2012). The Aghajari Formation displays two distinct facies. Sandstone facies are found in the Inner Fars region, near Bandar Abbas, north of the Dezful embayment, and along the Iran-Iraq border. Conversely, a marly facies is evident in the coastal Fars region and the middle and southern parts of the Dezful embayment. The lower boundary of the Aghajari Formation is gradual with the Mishan Formation; however, in Lorestan Province, where the Mishan Formation is absent, it directly rests on the Gachsaran Formation. The Bakhtiari Formation defines the upper contact, which can sometimes appear gradual and conformable or abrupt and disconformable.

The Aghajari Formation has the greatest thickness in the Dezful embayment but decreases towards the east and southeast (Amiri-Bakhtiar and Nouraee-Nezhad, 2022). The thickness of the Aghajari Formation decreases as the Mishan Formation increases; therefore, at times, the Aghajari and Mishan formations are considered to be the same, and the age of the Aghajari is assumed to be from the Middle Miocene to the Pliocene (Ghorbani, 2015). The age of the Aghajari Formation varies across different locations. This formation ages progressively from younger to older, from north to south. The Aghajari Formation is considered to have formed in lake, marine, bay, and river settings in the Khuzestan and Lorestan provinces (Bahrami, 2009; Gohari, 2014). In contrast, on the coastal Fars and Qeshm Island, it exhibits marine features (Moradi, 2014; Bahrami, 2009). The Lahbari member constitutes the upper part of the Aghajari Formation, distinct from its lower parts in terms of depositional environment, particle size, facies color, and sedimentary structures.

The goal of this research is to reconstruct the depositional environment of the Neogene Aghajari Formation in the Zagros region, located within the Lorestan sedimentary basin. Consequently, a relationship can be established between the depositional environment and aspects such as sequence stratigraphy, tectonics, and sea level changes.

2. Geographical and geological setting

The Afrineh syncline is one of the largest and broadest synclines in the Lorestan basin. It is 31 km long and 5 km wide, lying between the Amiran anticline to the northeast and the Sarkan anticline to the southwest (Motiei, 2012; Emami, 2008).

The convergence of the Arabian and Eurasian plates has led to the elevation of the Iran-Anatolia plate, which subsequently caused the closure of the Neotethys Sea during the Miocene-Pliocene (Agard et al., 2011; Vergés et al., 2019). The collision has created four structural zones in western Iran: the Persian Gulf foreland basin, the high Zagros zone, the Zagros folded-thrust belt, and the

Urumieh-Dokhtar zone. The studied area is located in the Lorestan Province and the folded Zagros zone (Fig. 1). The examined sections are situated in the Afrineh syncline, approximately 46 kilometers southwest of Khorram Abad city. These sections are located near Afrineh city, along the Khorramabad-Andimeshk highway. Fig. 2 illustrates the locations of the sections. The Asmari, Gachsaran, and Aghajari formations are cropped out in the Afrineh syncline. The Mishan Formation is absent, and the Aghajari Formation lies directly atop the Gachsaran Formation (Fig. 3). The Gachsaran Formation in the Zagros mountains exceeds 2000 meters in thickness and comprises gypsum, anhydrite, marl, and carbonate rocks deposited in a lagoon environment (Gill and Ala, 1972) between Oligocene-Miocene (Bahroudi and Koyi, 2004; Pirouz et al., 2015) and Lower-Middle Miocene (Jones and Racey, 1994). The depositional environment of the Gachsaran Formation in the studied area is attributed to subtidal, intertidal, lagoon, barrier, and enclosed to semi-enclosed marine environments (Sun et al., 2021).

The base of the Aghajari Formation has a diachronous age, ranging from the Middle to the Upper Miocene (Vergés et al., 2019). According to James and Wynd (1965), the age of the Aghajari Formation was determined through fossil evidence, dating from the late Miocene to the Pliocene.

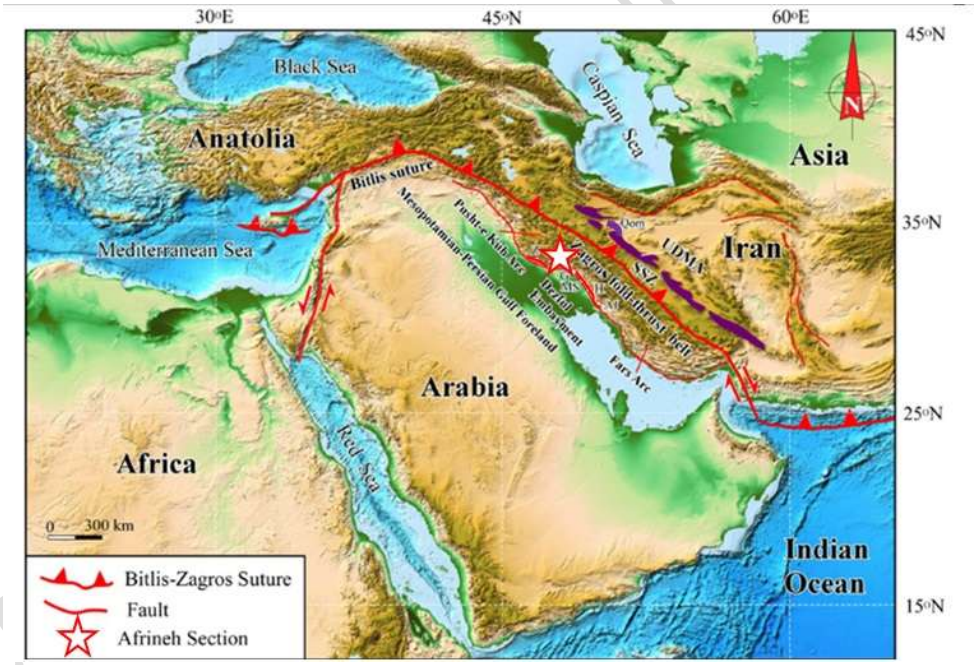

Figure 1. The tectonic position of the studied area (Afrineh syncline) is located in the Zagros folded thrust zone. This structural zone results from the collision between the Arabian and Eurasian tectonic plates, which was subsequently followed by the elevation of the Iran-Anatolian plate. (After Sun et al., 2021).

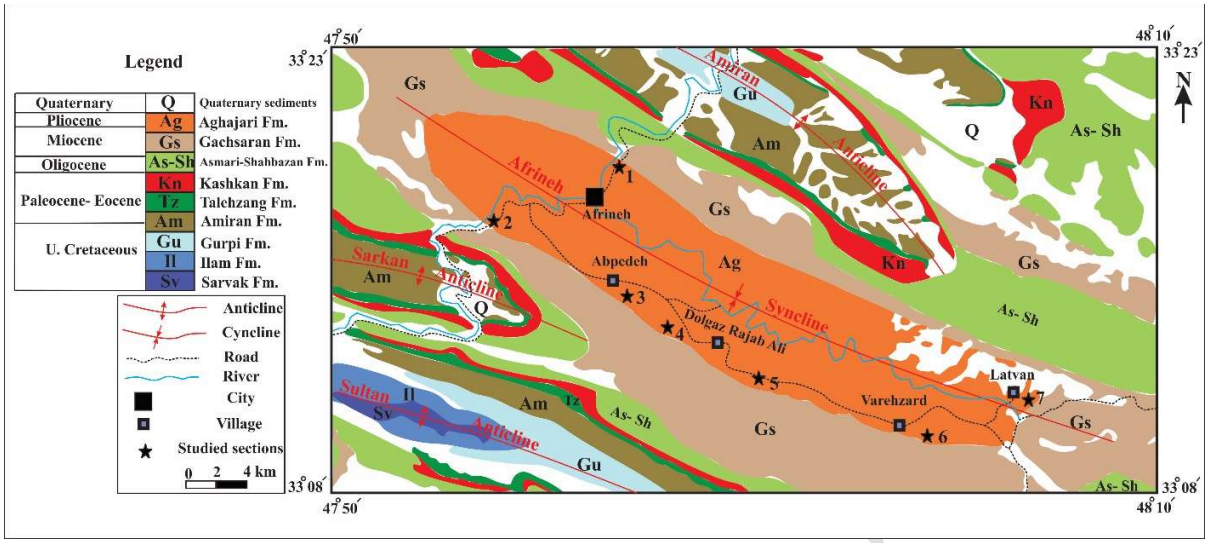

Figure 2. Geological map of Khorram Abad and Poldokhtar, along with the location of the Afrineh syncline and the extension of formations in the area (after Fakhari, 1985, with modifications). Asterisks indicate the study sections. (1 and 2: Afrineh section; 3: Abpedeh village section; 4 and 5: Dolgaz Rajab Ali village section; 6: Vareh-Zard village section; 7: Latvand Baraftab village section).

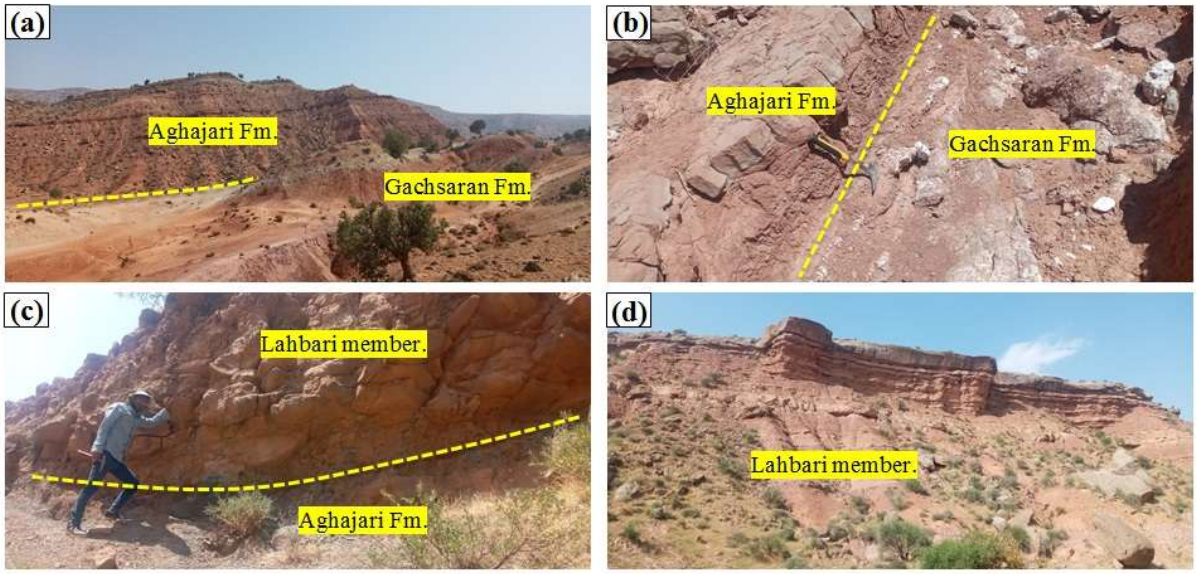

Figure 3. Field photograph of the existing strata in the Afrineh syncline. (a) Gachsaran and Aghajari formations (the lower part of the studied sections). (b) The sharp boundary between the Gachsaran and Aghajari formations. (c) The sharp boundary between the Aghajari Formation and the Lahbari member. (d) Lahbari member (the upper part of the studied sections).

3. Materials and methods

Seven sections were selected based on accessibility, thickness, facies variety, and least soil coverage (Table 1). The facies characteristics in the field have been thoroughly examined and documented, including their forms and lateral extensions, sedimentary structures, fossil contents, the nature of layer contacts, and sediment accumulation patterns. A total of three hundred samples were collected from all examined sections. Each sample was processed into a thin section and analyzed using an Olympus BH2 polarizing microscope at Bu–Ali Sina University. Miall's (2006) and Allen's (1964) facies codes, as well as Pettijohn's (1975) classification scheme, were employed to characterize the sandstones and mudstones. Carbonate facies are classified based on Dunham's (1962) system. Trace fossils are classified following Seilacher's (2006) approach. The depositional model for the Aghajari Formation within the Afrineh syncline has been established by integrating data from microscopic examinations, field investigations, lithofacies, and facies associations.

Table 1. Selected sections from the Aghajari Formation in Afrineh syncline

Section name	Geographic location	Thickness (meter)	Lithology
1- Afrineh (1)	N 33° 16′22.37″ E 48° 01′ 06.10″	550	Alternation of sandstone, siltstone, claystone, mudstone, shale, and, to a lesser extent, conglomerate.
2- Afrineh (2)	N 33° 13′ 14.3″ E 48° 00′ 40.32″	540	Alternation of sandstone, siltstone, claystone, mudstone, shale, and, to a lesser extent, conglomerate.
3-Abpedeh	N 33° 14′ 12.11″ E 48° 01′ 35.18″	520	Alternation of sandstone, siltstone, claystone, mudstone, shale, and, to a lesser extent, conglomerate.
4-Dolgaz RajabAli (1)	N 33° 13′ 24.10″ E 48° 04′ 22.30″	530	Alternation of sandstone, siltstone, claystone, mudstone, shale, and, to a lesser extent, conglomerate.
5- Dolgaz Rajab Ali (2)	N 33° 13′ 40.21″ E 48° 02′ 15.20″	590	Alternation of sandstone, siltstone, claystone, mudstone, shale, and, to a lesser extent, conglomerate.
6-Vareh-Zard	N 33° 12′ 25.10″	560	

	E 48° 04′ 21.30″		Alternation of sandstone, siltstone, claystone, mudstone, shale, and, to a lesser extent, conglomerate.
7-Latvand Baraftab	N 33° 13′ 38.9″ E 48° 06′ 51.00″	600	Alternation of sandstone, siltstone, claystone, mudstone, shale, and, to a lesser extent, conglomerate.

4. Lithofacies

Lithofacies reflect the mode of transport of sedimentary bodies, the energy of the water, and the mechanisms of deposition. They serve as an essential basis for understanding microfacies, recognizing genetic sand bodies, and defining units of reservoir architecture (Dongyang et al., 2019; Aigbadon et al., 2023). Field investigations across seven stratigraphic sections in the Afrineh syncline resulted in the recognition of eighteen lithofacies. The lithofacies consist of three types of conglomerate lithofacies (Gm, Gp, Gt), nine types of sandstone lithofacies (Sp, St, Sm, Sh, Sr, Sfl, Sl, Slr, Sr(Fl)), four varieties of mud lithofacies (Fm, Fl, Fcf, Fl(Sr)), a gray shale facies rich in planktonic fauna, as well as a bioclastic grainstone facies (Table 2.). The sequences also revealed the presence of Skolithos facies.

According to lithofacies and architectural elements, the Aghajari Formation in the studied area consists, from bottom to top, of Meandering rivers, tidal flats, deep and shallow marine environments, and Meandering and Braided rivers. Each setting is explained in detail below.

Table 2. Summary of the characteristics of the lithofacies types encountered in the Aghajari Formation.

Facies	Lithology	Sedimentary structure	Texture	Fossils	Contacts	Geometry	Extent and lateral relationships	Environmental interpretation
Gm	Conglomerate and coarse sandstone	Massive characteristics, though it occasionally shows faint layering	Matrix-supported conglomerate, typically displaying massive characteristics, clasts range from sub-angular to sub-rounded, with some showing significant rounding.	None	The lower boundary of this facies is abrupt and erosional, whereas the upper boundary may be abrupt or gradual	Thick, lenticular to tabular	Usually 1-6 m in lateral extent	longitudinal bars in braided rivers, gravelly sheets, and channel deposits. Longitudinal bars in the gravelly rivers
Gp	Conglomerate and coarse sandstone	Planar cross-stratification	Grain-supported clasts range from sub-angular to sub-rounded	None	The lower and upper boundaries of Gp are erosional	Thick, lenticular to tabular	Usually 1-3 m in lateral extent, low-angle, wedge-shaped lateral pinch-out	Deeper parts of a braided river channel
Gt	Conglomerate and coarse sandstone	Trough cross-stratification	Grain-supported or matrix-supported, poor sorting, with particle sizes varying from granule to pebble.	None	The lower boundary of this facies shows good symmetry.	Thick, lenticular to tabular	Usually 1-3 m in lateral extent	Migrating three-dimensional gravel bars in braided rivers
Sp	Fine to coarse sandstone	Planar cross-stratification	Particles in this facies range from fine to coarse sand, medium roundness, and sorting; they are texturally immature to sub-mature.	None	The facies Sp transitions vertically into facies Sh with a distinct and flat contact surface	Thin, lenticular to irregularly wedge-shaped	Sand bodies extend over tens of meters, wedge-shaped lateral pinch-out	Migration of two-dimensional ripples and dunes in meandering rivers.
St	Fine to coarse sandstone	Trough cross-stratification	Particles in this facies range from fine to coarse sand, medium to well-rounded and indicate a textural range from sub-mature to mature	None	Sharp boundaries between individual sets and cosets.	Thin, lenticular, or wedge-shaped	Sand bodies extend over tens of meters, wedge-shaped lateral pinch-out	Migration of three-dimensional ripples and dunes in the braided and meandering river
Sm	Moderate to fine-grained sandstone	Massive characteristics, though it occasionally shows faint layering	Particles in this facies range from moderate- to fine-grain sand; grains are poorly to well sorted and well-rounded to subrounded in texture.	None	This facies may or may not show an erosive lower surface, but the upper surface is commonly sharp and often	Thin, lenticular to tabular	Thickness varies from 20 cm to 2 m and maintains Lateral continuity between 1 and 10 m.	This lithofacies is commonly found in the channels of meandering rivers and the crevasse splay deposits.

					undulatory or irregular			
Sh	Very fine to Medium Sandstone.	Horizontally stratified	The grain size ranges from very fine to medium sand. These sediments exhibit fairly good sorting and roundness, and regarding textural maturity, they are classified as sub-mature to mature	None	Facies Sh has been vertically transformed into Sr, Sp, Sm, and St lithofacies. The upper and lower boundaries of the facies are sharp.	Thin, tabular	The bounding surfaces may be traced for tens of meters	This facies could be deposited via high-energy sheet floods that spilled into a lower energy environment from channels during flooding of the main fluvial channel system.
Sr	Fine to medium sandstone	Ripple cross-laminated	The sandstone grains range from fine to medium, exhibiting medium to fairly good rounding and sorting.	None	The lower boundary is sharp and erosional with facies Sp, and the upper boundary is sharp with facies Sh, Fl, or Fm.	Thin, lenticular, or wedge-shaped	Sand bodies extend over tens of meters, wedge-shaped lateral pinch-out	The upper part of bedforms and bars, crevasse splay deposits in overbank areas.
Sfl	Fine to medium sandstone	Flaser-laminated	The sandstone grains range from fine to medium, well-sorted and well-rounded. .	Rare	The lower boundary is with facies Sh, and the upper boundary is sharp with facies Sh, Fl, or Fm.	Thin, tabular	Sand bodies extend over tens to hundreds of meters.	Lower intertidal subenvironment
Sl	Fine to medium sandstone	Ripple cross-laminated	The sandstone grains range from fine to medium, medium to fairly good rounding and sorting.	Rare	The lower boundary is with facies Sp and Fm, and the upper boundary is sharp with facies Fl or Fm.	Thin, lenticular, low-angle cross-lamination (less than 10°)	Sand bodies extend over tens of meters, wedge-shaped lateral pinch-out	Channels of a meandering river.
Slr	Fine to medium sandstone	Ripple cross-laminated	The sandstone grains range from fine to medium, medium to fairly good rounding and sorting.	Rare	The lower boundary is with facies Fm; the upper boundary is sharp with facies Fl or Fm.	Thin, tabular, low-angle cross-lamination	Sand bodies extend over tens of meters, wedge-shaped lateral pinch-out	Channels of a meandering river.
Sr(Fl)	Sandstone	Sand ripples containing laminated mud.	The sandstone grains range from fine to medium, exhibiting medium to fairly good rounding and sorting.	Rare	The lower boundary is sharp with facies Sh, and the upper boundary is sharp with facies Sh, Fl, or Fm.	Thin, sheet-like packages	Lateral extent, which can commonly be traced over 200 meters.	Tidal flat environment
Fm	Fine-grain mudstone	Massive, poorly laminated structures	This facies mainly consists of siltstone, homogeneous mudstone and minor portion of fine to	None	Due to the underlying topography, the lower boundary is commonly flat and irregular; the	Thick, sheet-like packages	Broad lateral extent, which can commonly be traced over 1000 meters.	Meandering rivers overbank and floodplain

			coarse-grained sandstone		upper boundary is erosional with St facies.			
Fl	Fine-grain mudstone	Parallel laminated structures	This facies mainly consists of siltstone and claystone,	None	The lower and upper bed boundaries are generally sharp and planar	Thick, sheet-like packages, rarely wedge-shaped.	Broad lateral extent, which can commonly be traced over 300 meters.	Meandering rivers overbank and floodplain
Fcf	Fine-grain mudstone	Massive, poorly laminated structures	This facies mainly consists of siltstone, homogeneous mudstone and minor portion of fine to coarse-grained sandstone	None	The lower boundary is commonly flat and irregular due to the underlying topography; the upper boundary is erosional with St facies.	Thick, sheet-like packages	Broad lateral extent, which can commonly be traced over 1000 meters.	Meandering rivers overbank and floodplain
Fl(Sr)	Mudstone	Laminated mud containing sand ripples	This facies mainly consists of siltstone and claystone with sand ripples	Rare	The lower boundary is with facies Sh, and the upper boundary is sharp with facies Sh or Fm.	Thin, sheet-like packages	Lateral extent, which can commonly be traced over 200 meters.	Tidal flat environment
Shale	Shale	Lamination	Medium to fairly sorting.	Rich in planktonic fauna	The lower boundary is sharp with facies Fm, and the upper boundary is sharp with facies Sr, Fl, or Fm.	Thick, sheet-like packages	Lateral extent is restricted	Deep marine
Bioclast grainstone	Bioclast grainstone	Layering	Grain supported with intergranular calcite cement.	Rich in bivalves, echinoderms, and small gastropods	The lower boundary is sharp with facies Fm, and the upper boundary is sharp with facies Sr, Fl, or Fm.	Thin, sheet-like packages	Lateral extent is restricted	Shallow marine

4.1. Facies association in the lower to middle part sections

Sandstone lithofacies

Sandstone facies within depositional environments arise from the movement of sand by traction currents, either as bed load or saltation load (Miall, 1996; Stow et al., 2020). Medium-grained sandstone facies are particularly prevalent due to their formation in various flow regimes (Tucker, 1991). A total of seven sandstone facies were recognized within the meandering river setting, comprising ripple sandstone lithofacies (Sr), ripple cross-lamination (Slr), horizontally stratified (Sh), planar cross-lamination (Sp), trough cross-stratification (St), massive (Sm), and low-angle

cross-lamination (Sl). In these lithofacies, chertarenite and calclitharenite have been recognized alongside sandstone petrofacies.

Ripple cross-laminated sandstone facies (Sr)

Description

The Ripley sandstone facies (Sr) is commonly found in sandstone deposits and displays a significant prevalence. The sandstone grains range from fine to medium, exhibiting medium to fairly good rounding and sorting. A main feature of these lithofacies is the occurrence of various types of asymmetric ripple marks (current ripple), including straight and sinuous-crested, linguoid ripples, and climbing ripples (Fig. 4). The X-ripple lamination shown in Fig. 4e developed during the movement of ripples. These submature sandstones consist of chertarenite and calclitharenite petrofacies (Fig. 4).

Interpretation

The asymmetrical current ripples and cross-lamination covered by clay layers suggest that deposition occurred through alternating subaqueous traction and suspension (Miall, 1996). This facies likely indicates a temporary halt in bar migration, resulting from either the receding floodwaters or deposition in areas with slow-moving or stagnant water between bars or overbank zones (Bose and Chakraborty, 1994; Zamaniyan et al., 2021). Facies Sr may be linked to the downstream movement of asymmetrical ripples in meandering rivers under controlled sediment supply conditions in a lower, low-intensity flow regime (Allen, 1983). Consequently, this facies reflects gradual sediment accumulation within mostly inactive channels, resulting in fill deposits (Miall, 1996).

Figure 4. Types of ripples found in the Aghajari Formation. (a) Asymmetrical ripple with straight and bifurcated crescents. (b) Linguid ripples. (c) Climbing ripples. (d) sinuous-crested ripples. (e) X-Ripples formed in the medium-grained sandstone. (f) An example of a small-scale ripple (black arrow) formed inside a sandstone. (g) Coarse-grained sandstone (calclitharenite) is found in the lower part, and (h) Fine-grained sandstone (calclitharenite) is found in both the lower and middle parts of the Aghajari Formation.

Ripple cross-lamination facies (Slr)

Description

Lithofacies Slr consists of fine- to medium-grained sandstone characterized by ripple cross-lamination. In addition to the cross-lamination, siltstone layers are also seen (Fig. 5). The ripples are asymmetric, suggesting the direction of the current from right to left (northeast to southwest). These sandstones fall into the submature category and are identified as chertarenite petrofacies. The main difference between the Slr and Sr lithofacies is their characteristics: Sr lithofacies presents sandy formations with ripples, while Slr lithofacies does not exhibit these ripple structures.

Interpretation

This facies is interpreted as a sediment suspension over the upper parts of sandy bedforms or across low-relief, abandoned floodplains (Allen, 1964). The internal structures of this facies are distinguished by unevenly wavy lamination and thin mud lamina atop the sandy beds. A few asymmetrical and symmetrical ripples can be observed.

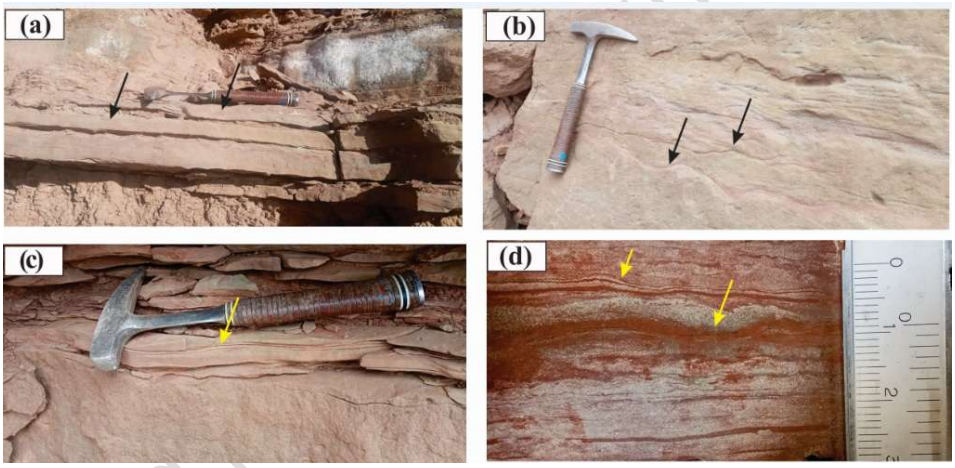

Figure 5. (a) Ripple cross-lamination observed in finely laminated sandstone; (b) Ripple cross-lamination created in the medium-grained sandstone layer. (c) Ripple cross-lamination was identified in the fine-grained sandstone layer. (d) A ripple cross-lamination example is shown after the hand specimen of sandstone was polished (indicated by yellow arrows).

Horizontally stratified sandstone facies (Sh)

Description

This lithofacies is prominently present in the sections examined. It appears as thin laminae, creating a sequence that varies in thickness from several centimeters up to a maximum of 1.5 meters (see Fig. 6). The grain size ranges from very fine to medium sand. These sediments exhibit fairly good sorting and roundness, and regarding textural maturity, they are classified as sub-mature to mature. Their petrofacies consist of chertarenite and calclitharenite. Facies Sh has been vertically transformed into Sr, Sp, Sm, and St lithofacies. In the river channels, the horizontal

laminations are associated with an upper flow regime, while cross-laminations indicate a lower flow regime. Within the analyzed lithofacies, the horizontal laminations at the base have evolved into trough cross-laminations in the upper section, indicating a reduction in flow energy as one moves upward through the sequence (Fig. 7a and b). In Figure 6d, voids aligned with the plane of the lamination (yellow dashed line) can be seen. These are remnants of granules and mud clasts that have been excavated.

Interpretation

Lithofacies Sh can develop in higher and lower flow regimes (Boothroyd and Ashley, 1975; Harms et al., 1982; Allen, 1984; Miall, 1996; Jo et al., 1997; Lee and Chough, 2006).

Consequently, coarse-grained sandstone facies emerge under an upper-flow regime, while fine-grained sandstones are formed in a lower-flow regime (Miall, 1985 and 2000).

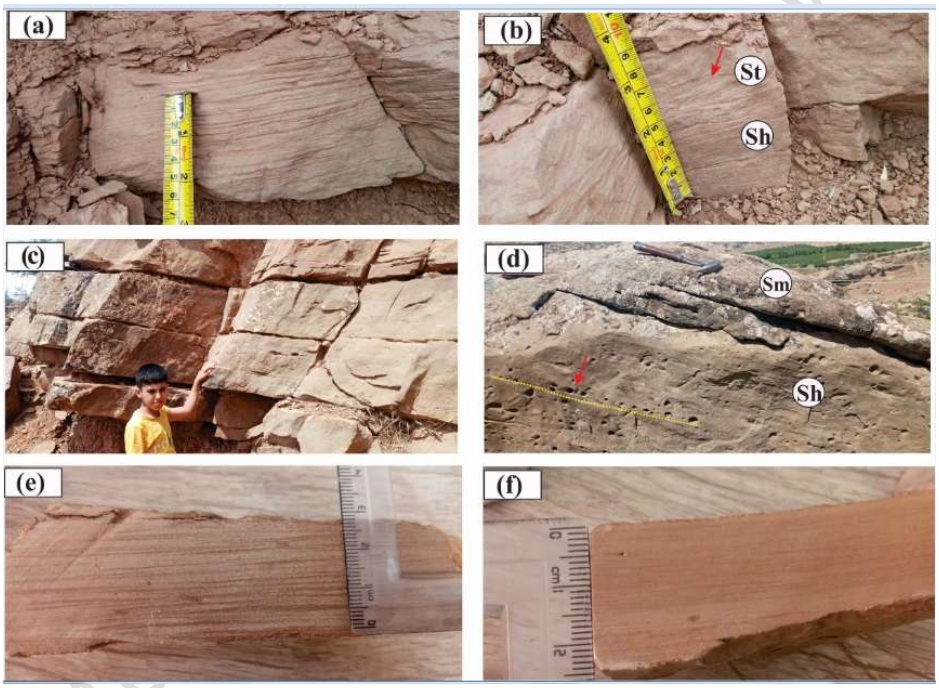

Figure 6. (a) Horizontal lamination caused by alternating sand and silt. (b) The horizontal laminae in the lower section, marked by the red arrow, changed into trough-cross laminae at the upper section. (c) Horizontal bedding in medium to thick-layered sandstones. (d) Horizontal laminations (Sh) are present at the bottom (red arrow), while the upper section has transitioned into massive sandstone (Sm). (e) and (f) Illustrations of fine-scale sedimentary structures (microstructure) of horizontal laminations that can be seen after polishing the cut surface.

Planar cross-stratified sandstone facies (Sp)

Description

The facies Sp transitions vertically into facies Sh with a distinct and flat contact surface (Fig. 7). The particles of this lithofacies exhibit medium roundness and sorting, indicating textural immaturity to submaturity. The migration of two-dimensional ripples and dunes plays a significant

role in the development of these facies. The petrofacies of the lithofacies consist of chertarenite and calclitarenite.

Interpretation

This lithofacies features planar cross-stratification, signifying that unidirectional currents formed it during deposition. (Tucker, 2001; Longhitano et al., 2012; Davis, 2012). The particles in this facies range from fine to coarse and primarily develop in lower flow regime conditions, characterized by two-dimensional mega ripples and ripples (Harms et al., 1982; Miall, 1985; Strand, 2005; Therrien, 2006).

Trough cross-bedded sandstone facies (St)

Description

This lithofacies is defined by its trough cross-stratified, fine- to coarse-grained sandstones. In the lower and middle sections of the sequences, fine- to medium-grained sandstones exhibit small-scale brown-red trough laminations, whereas the upper sections reveal coarse-grained gray sandstones featuring larger-scale trough laminations in the Lahbari member. The thickness of each set of trough cross-lamination typically ranges from 10 to 50 cm and can extend laterally up to 1 m (Fig. 7). The grains in this facies are medium to well-rounded and indicate a textural range from sub-mature to mature. Chertarenite and calcarenite are the identified petrofacies.

Interpretation

Lithofacies St typically develops in a lower flow regime (Harms et al., 1982; Miall, 1985) as a result of the migration of three-dimensional ripples and dunes (Miall, 1996; Gani and Alam, 2004; Therrien, 2006; Ghosh et al., 2006).

Low-angle cross-lamination sandstone facies (Sl)

Description

This lithofacies appears brown-red with a lenticular shape (see Fig. 8). It is characterized by low-angle cross-lamination (less than 10°) and is predominantly found in the lower and middle sections of the studied area.

Interpretation

This lithofacies develops in lower and upper flow regimes (Boothroyd and Ashley, 1975; Harms et al., 1982; Allen, 1984; Miall, 1996; Jo et al., 1997; Miall, 2000). Nonetheless, it is predominantly created under conditions of higher velocity and low sediment load (Harms et al., 1982; Miall, 2000). Facies Sl is indicative of unidirectional traction currents or the movement of ripple marks (Tucker, 1991). Based on the sedimentary structures present and the geometry of the strata, it can be inferred that these sandstones were deposited in the channels of a meandering river.

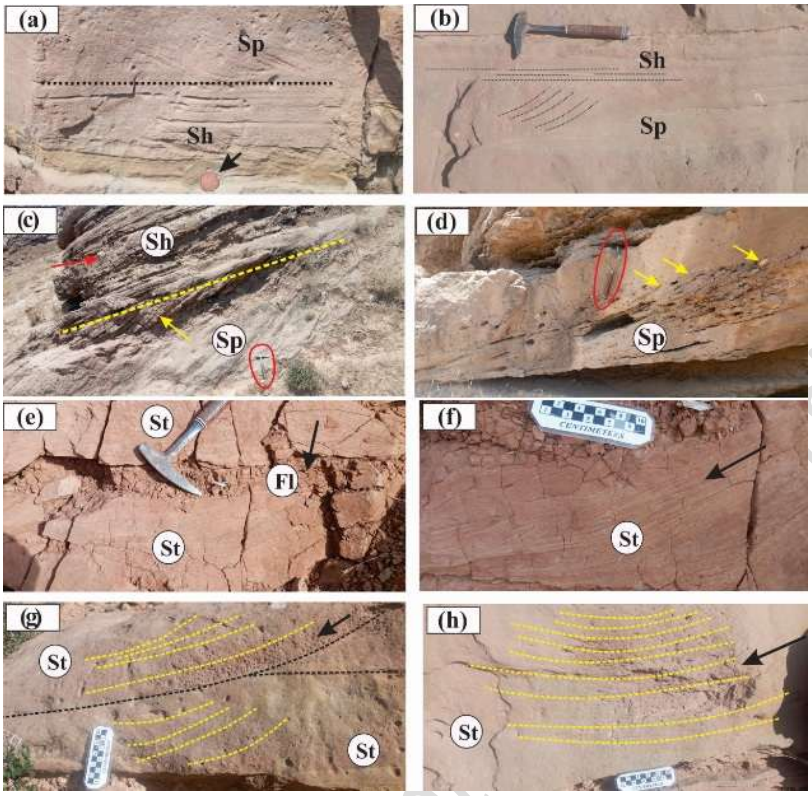

Figure 7. (a), (b), and (c) The interchange of Sp and Sh signifies variations in energy and flow velocity. The coin is observed as a scale (black arrow); (d) Low-angle planar cross-bedding (15 to 20°). Gravel and mud fragments (yellow arrows) are present on the surface of the lamination. (e) Fine-grained mud between the facies St (black arrow); (f) a close-up view of (e), the arrow shows the flow direction; (g) and (h) Two sets of St facies.

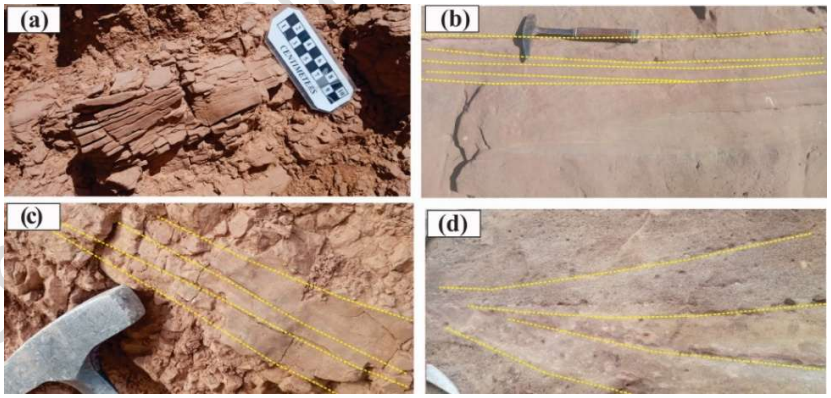

Figure 8. Field photos of low-angle cross-stratified sandstone (Sl).

Massive sandstone facies (Sm)

Description

This lithofacies features sand that ranges from moderate to fine grain size, with a channel- or lens-shaped structure. Thickness varies from 20 cm to 2 m and maintains lateral continuity between 1 and 10 m (Fig. 9). Toll marks can be seen on the surfaces of the layers (Fig. 9-f), and convolute

bedding is present within sandstone beds in facies Sm (Fig. 9-e). This lithofacies is found chiefly between the talweg and point bar, as well as in crevasse splay and levees. In the upper part, it ends in sandstone with a parting lineation characterized by a high Froude number. These sandstones are immature to submature and consist of calclitharenite petrofacies.

Interpretation

The absence of internal structure has been attributed to a plentiful sediment supply and currents that carry a significant sediment load (Miall, 2000; Tucker, 2003). This lithofacies is commonly found in the channels of meandering rivers and the crevasse splay deposits in the lower parts of the studied sequence. The erosion of channel banks and the rapid accumulation of sediment in these rivers contribute to the absence of internal structures in the deposits (Miall, 2000). Facies Sm has also been attributed to quick deposition from suspension in upper flow regimes (Harms et al., 1982; Reading, 1996; Miall, 1996).

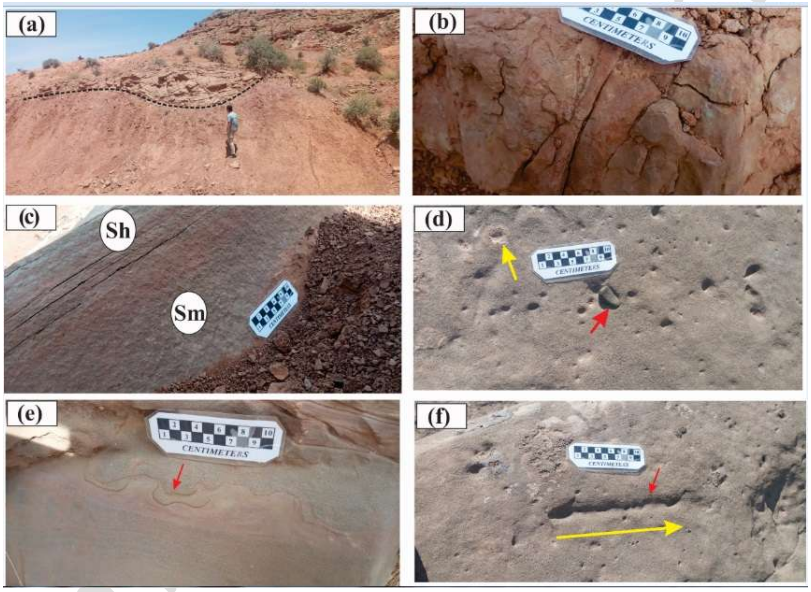

Figure 9. (a) Meandering channel with Sm lithofacies; (b) A close-up of (a); (c) Massive sandstone facies changes vertically into horizontally laminated facies (Sh); (d) The top surface of facies Sm displays traces of gravel; (e) convolute bedding (red arrow); (f) the tool's path on the bedding surface, indicated by the red arrow.

Fine-grained facies Association

The studied sections predominantly revealed fine-grained lithofacies, which comprise over 60% of the sequences in the lower and middle regions of the Aghajari Formation. Three siltstone and mudstone facies were recognized in these areas: Fm, Fl, and Fcf.

Parallel laminated siltstone and claystone facies (Fl)

Description

In all the sections studied, the Aghajari Formation sequence begins with laminated mud facies placed on the Gachsaran Formation (Fig. 10). The mudstones at the boundary between the Aghajari

and Gachsaran formations have a thickness ranging from 20 to 50 cm. This facies is frequently seen in overbank and floodplain settings, mainly in the lower and upper parts of the studied sequences. This lithofacies displays small-scale sedimentary features (micro-structures) like lamination and concretions. Microscopic photographs of these features are presented in Fig. 12-e and f. The concentration of iron oxide along the laminations suggests that this lithofacies formed under oxidizing conditions (in a continental environment).

Interpretation

This lithofacies consists of particles ranging in size from silt to clay, primarily deposited from suspension (Higgs et al., 2012; Powell et al., 2016). It is distinguished by its fine and parallel laminae, which typically display red-brown colors. The red color results from the oxidizing conditions in the depositional environment (Davis, 2012; Zamaniyan et al., 2018).

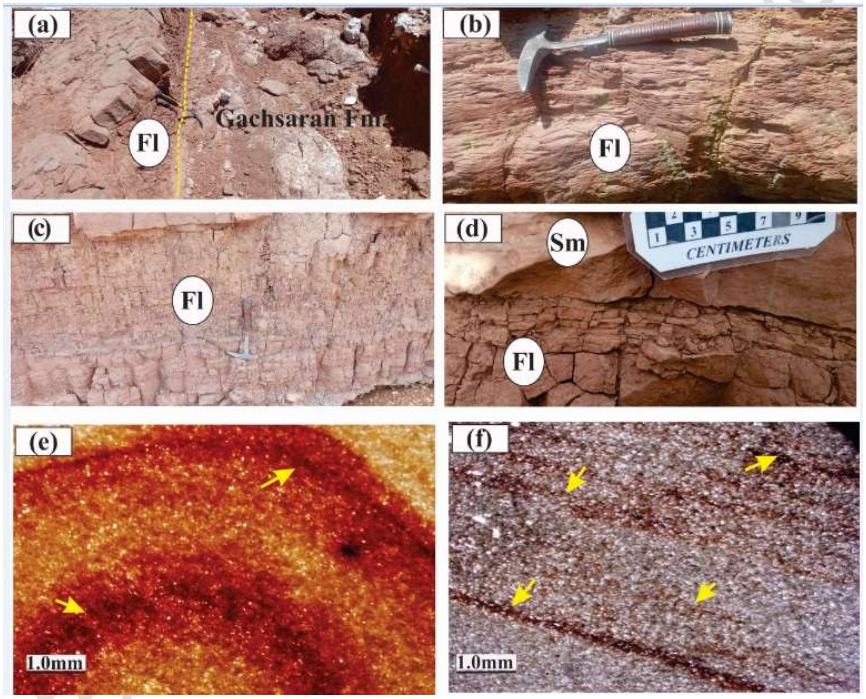

Figure 10. Laminated mudstones (a) located at the base of the Aghajari Formation; (b) mudstones with the presence of concretions; (c) and (d) facies Sm lies above Fl on an erosional surface (yellow arrow). (Sm: Massive sandstone lithofacies; Fl: Laminated mudstone). e: Mudstone lithofacies with concretion structure. f: Mudstone lithofacies with lamination structure.

Massive mudstone facies (Fm and Fcf)

Description

These lithofacies are massive and arranged in thick beds, exceeding 5 m in thickness (Fig. 11). They exhibit red-brown and purple colors. Concretions are commonly found as diagenetic sedimentary structures. Lithofacies Fcf primarily consists of mudstone characterized by massive structures.

Interpretation

They are associated with other fine-grained facies, suggesting the rapid deposition of suspended particles in a low-energy setting, such as floodplains in fluvial environments (Woo et al., 2006; Miall, 2006). These lithofacies are interrupted by river-channel facies and possess significant thickness, suggesting they may have developed within a meandering river floodplain (Miall, 1977).

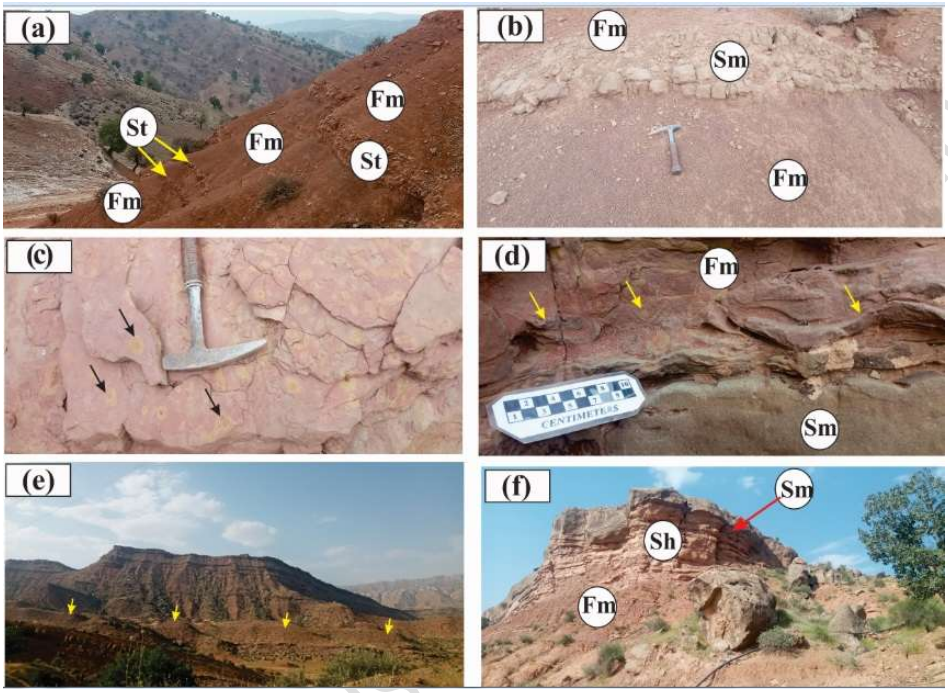

Figure 11. Massive mudstone layers are found in the lower section of the Aghajari Formation. Sandstone interlayers and lenticular bodies are visible. In (a), the field photo has a width of 80 meters, whereas in (e), it measures 850 meters, and in (f), it is 130 meters.

4.2. Facies association in the middle part of the sections

This facies association occurs in the lower intertidal, upper intertidal, and, to a lesser extent, upper subtidal subenvironments. Interference and wavy ripples, flaser bedding, and mudstones intersected by small and minor sandy channels indicate upper sub-tidal, inter-tidal, and upper intertidal areas, respectively.

Upper subtidal subenvironment

Ripple sandstone lithofacies (Sr)

Description

Ripple lithofacies (Sr) are present in shallow marine settings influenced by tidal activity. These lithofacies comprise fine- to medium-grained, well-sorted, and well-rounded sandstones and consist of chertarenite and calclitharenite petrofacies. Symmetrical and interference ripples are recognized as features of shallow marine settings. The lithofacies Sr, accompanied by lenticular,

wavy, and flaser beddings (Fig. 12), indicate their development in tidal shallow marine sands. The usual thickness of individual units varies between 0.5 and 1 meter and typically spans 50 to 100 meters in lateral extent.

Interpretation

Symmetrical ripples (straight-crested) occur in shallow near-coastal areas within the wave agitation zone (Dalrymple et al., 1992), while interference ripples are related to tidal activity. They indicate they are created under varying flow regime conditions (Longhitano et al., 2012).

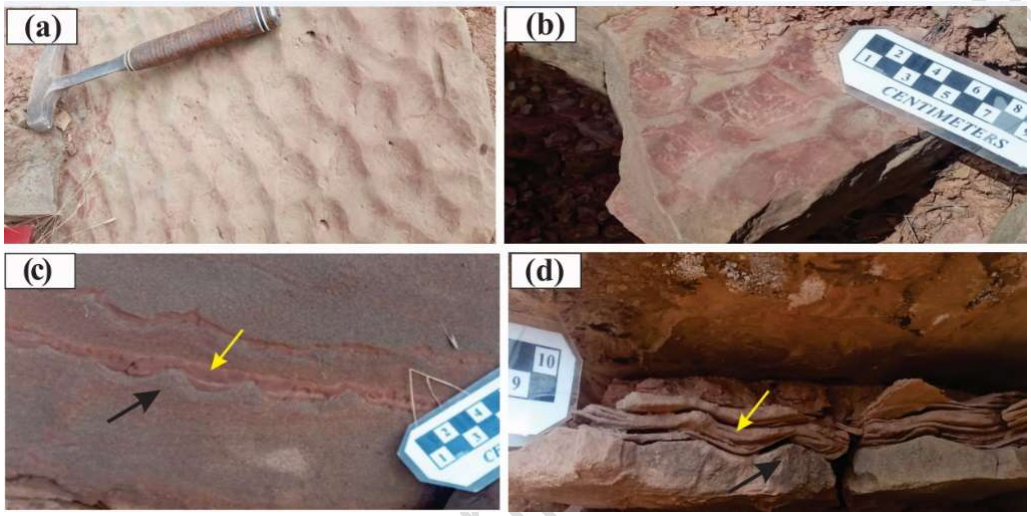

Figure 12. Ripple sandstone lithofacies: (a) and (b) interference ripples; (c) and (d) symmetrical ripple sandstone lithofacies. (The black arrows point to the symmetrical ripple, and the yellow arrows indicate the laminated mudstone formed on the ripples.)

Lower intertidal subenvironment

Sandstone flaser laminated lithofacies (Sfl)

Description

Figure 13 illustrates the sedimentary structures created by tidal action. In Fig. 13a and b, the change from wavy to lenticular bedding indicates a decrease in tide energy within the environment. This lithofacies exhibits sandstone petrofacies characterized by a significant presence of chert and carbonate lithics, featuring well-sorted grains (Fig. 13). The typical thickness of individual units generally ranges from 0.5 to 1.5 meters. It typically spans 50 to 100 meters in lateral extent.

Interpretation

Flaser, wavy, and lenticular beddings are typical features in shallow marine environments influenced by tides (Bhattacharya and Chakrabarty, 2000).

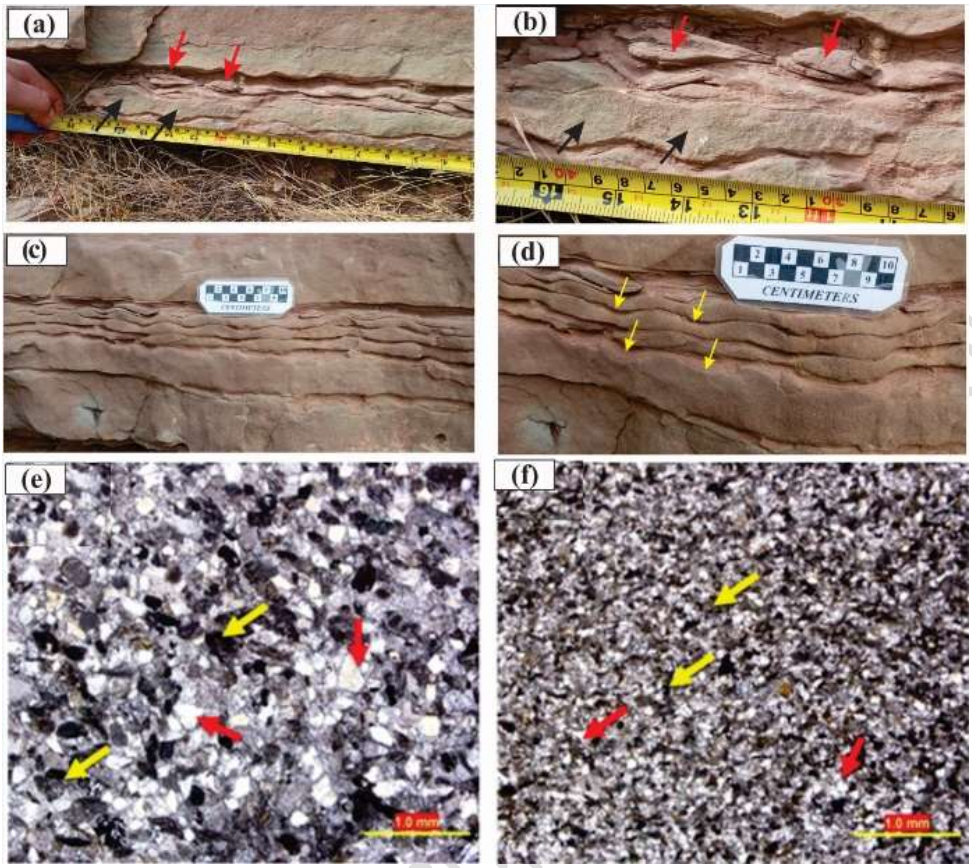

Figure 13. (a) and (b) Wavy (black arrows) and lenticular beddings (red arrows) formed in the tidal flat setting; (c) and (d) flaser bedding. (e) and (f), photomicrograph of well-sorted and rounded sedarenite petrofacies. (Red and yellow arrows show chert and carbonate rock fragments, respectively)

Fine-grained lithofacies with Fl (Sr)/ Sr (Fl) sandstone interlayers

Description

Two different lithofacies, including Fl(Sr) (laminated muds containing sand ripples) and Sr (Fl) (sand ripples containing laminated muds), are included in this association (Figure 14a-d). The sandstones are classified as immature to submature and comprise chertarenite and calclitharenite petrofacies. Individual units typically measure between 0.5 and 3.5 meters in thickness and extend laterally from 10 to 15 meters in length.

Interpretation

These lithofacies are formed due to changes in the energy level within depositional systems (Zand-Moghadam et al., 2014). As a result, low energy forms mud facies (lithofacies Fl), and high energy forms sand facies (lithofacies Sr) (Fig. 14). Flaser and lenticular bedding within these facies suggest the presence of tidal flat environments. When the water is stagnant (slack water), suspended mud settles on the crests of small ripples created on the sands after the water's velocity drops to zero. (Longhitano et al., 2012).

Upper intertidal subenvironment

Sandstone trough cross-stratification facies (St)

Description

This lithofacies is frequently found in meandering river environments, although it also occurs in smaller quantities within tidal channel settings. A notable feature of this lithofacies is the alternating clay and sand laminations in trough cross-beds, which are commonly observed in tidal channel areas (Fig. 14e-h). The particle sizes within the lithofacies vary from fine to medium sand, with occasional coarse sand exhibiting moderate to good sorting and rounding. These are typically classified as sub-mature to mature, showing lithofacies of chertarenite and calclitharenite. Fig. 14-g depicts a set of cross-laminations that display reactivation surfaces. The main characteristics of this environment include a prevalence of clay-rich sediments and minor sand bodies, which exhibit cross-stratification. Typical dimensions of individual units range from 0.5-1m in thickness and usually 3-5 m in lateral extent.

Interpretation

Mud laminations within sandstone (mud drape) suggest they were formed in a tidal environment typically found near coastal areas (Selley, 2000). Tidal channels often exhibit a lens-like geometry, characterized by an eroded base, limited lateral extension, and a maximum depth of approximately one meter. The essential features of this facies are a gently eroded surface, lateral accumulation, channel geometry, lens-like shape, and the presence of reactivation surfaces, which suggest sedimentation occurred within a tidal channel (Miall, 1992).

Ichnofacies

In every examined section, a single ichnofacies was identified, referred to as the Skolithos ichnofacies, which is detailed and interpreted in the following section.

Skolithos ichnofacies

Description

This ichnofacies contains an association of trace fossils of Lockeia (Lockeia isp), which relates to bivalve burrowing in sandy environments, as well as traces from Costa and Polycipes shells, traces of Planolites (Planolites isp), created by worm-like burrowing creatures, traces of Ophiomorphs (Ophiomorphs isp), related to crab burrowing in coastal areas, traces of Paleophycus (Paleophycus isp), and traces of Taenidium (Taenidium isp) have been noted (Fig. 15).

Interpretation

Skolithos ichnofacies were recognized in specific layers classified as shallow marine sandy shores (Seilacher, 2006).

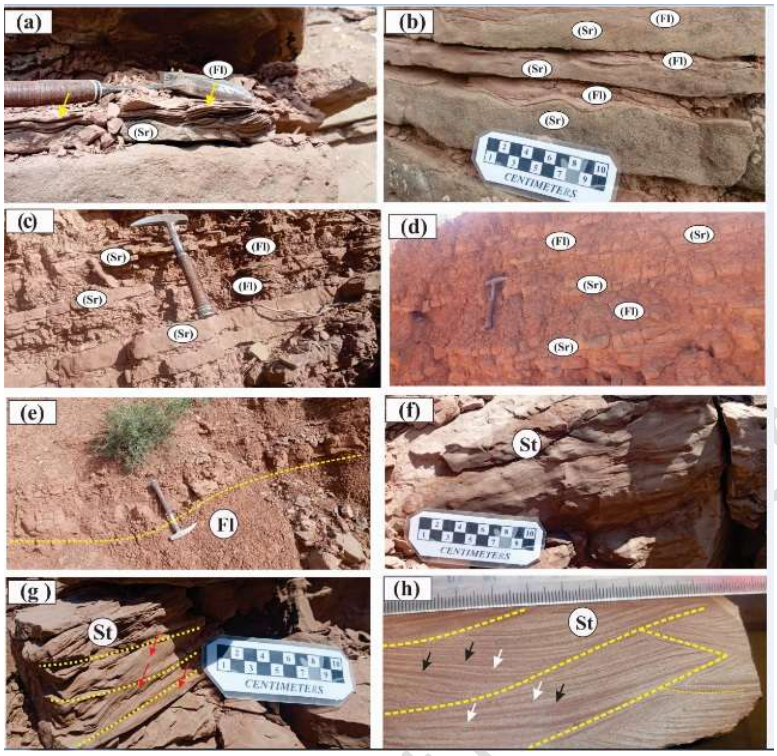

Figure 14. (a) and (b) Sr (Fl) lithofacies. The patterns created by ripples influence the formation of mud laminae; (c) and (d) Fl (Sr) laminar mudstone facies containing rippled sands. (e) Tidal channel facies with a lenticular shape and an erosional base; (f) a close-up view of the (e); (g) Cross-laminations (red arrows) are enclosed by reactivation surfaces (yellow dashed lines); (h) A close-up view of the polished surface of the sample showed in (g), Reactivation surfaces (yellow dashed lines) and mud drapes (black arrows) can be observed.

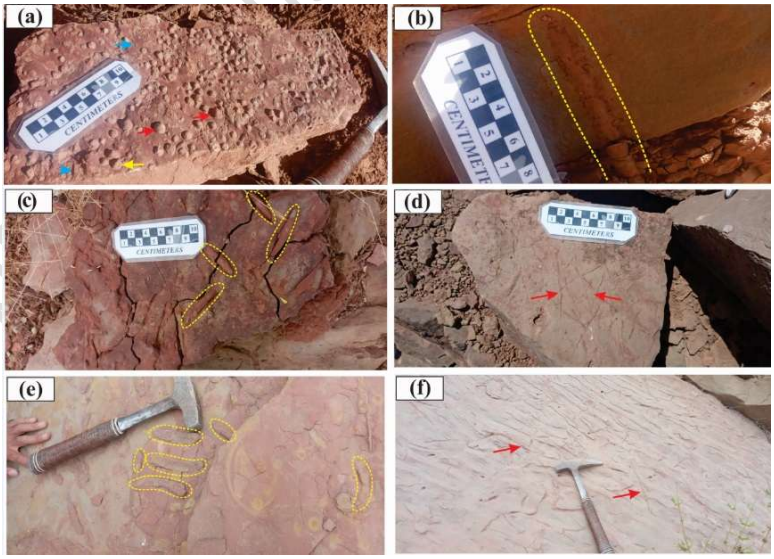

Figure 15. Trace fossils associations from shallow sandy shores: (a) Lockeia (Lockeia isp) (yellow arrow), Costa and Polycipes (red arrows), Planolites (Planolites isp) (blue arrows). (b) Ophiomorphs (Ophiomorphs isp); (c) Paleophycus (Paleophycus isp); (d) Planolites (Planolites isp); (e) and (f) Taenidium (Taenidium isp).

Biostratigraphy

Due to the clastic lithology of the studied sequences in the Agajari Formation, the fossil content within this formation is limited. The only fossils that have been identified include *Trilobatus primordius*, *Globigerinata*, Echinoderm stem, Bolivina (d'Orbigny, 1839), cf. ammonia, *Ammonia beccarii* var. tepida (Cushman, 1926), *Elphidium excavatum* (Terquem, 1875), *Elphidium* sp., and *Ammonia* sp. (Figs 16 and 17). These fossils have extensive ranges and do not indicate a specific age.

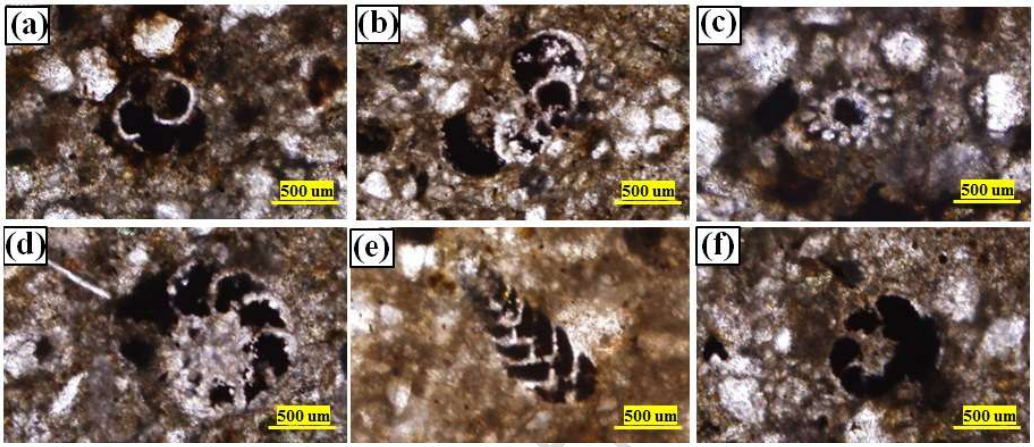

Figure 16. Photomicrograph of the gray shale and the marine fossils in this layer. (a) Trilobatus primordius; (b) Globigerinata; (c) Echnoderm stem; (d) Ammonia; (e) Bolivina d'Orbigny, 1839; and (f) cf.ammonia.

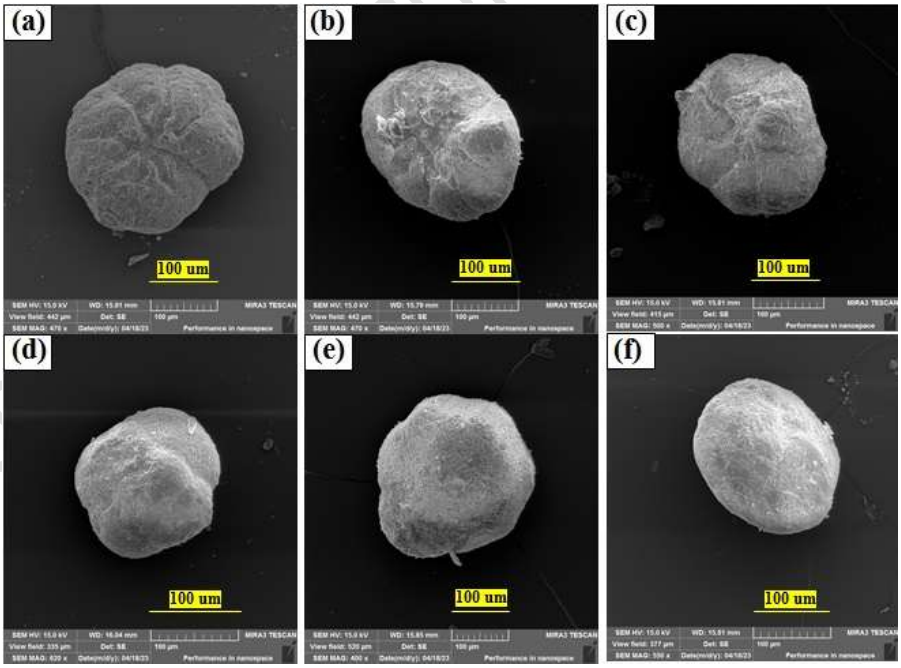

Figure 17. Scanning Electron Microscope images of the microfossils present in the gray shale unit. (a) Ammonia beccarii var. tepida Cushman, 1926 (umbilicus view); (b) Elphidium excavatum (Terquem, 1875); (c) Elphidium sp.; (d) Ammonia beccarii var. tepida Cushman, 1926 (spiral view); (e) and (f) Ammonia sp.

Deep marine facies association

Gray shale facies containing marine fauna

Description

This gray shale layer acts as a reference bed across the study area. Its thickness varies between 6 and 10 meters and contains very thin sandstone (chertarenite) interlayers (Fig. 18a-d). This unit occurs in the middle of the Aghajari Formation and is rich in marine fauna (Refer to figs 16 and 17). Following the regression of the sea and the development of a shallower basin environment, interbedded sandstone and bioclastic grainstone formed. The thickness of the sandy interbeds can reach up to 20 centimeters; however, their lateral extent is restricted.

Interpretation

Gray shales, rich in planktonic fauna, developed during sea transgression and increased basin depth.

Shallow marine facies association

Bioclastic grainstone microfacies

Description

This microfacies can be observed in the field as layers varying from a few centimeters to a maximum of 1.5 meters, which overlie the marine shale unit. It consists of bioclastic grainstones containing bivalves, echinoderms, and small gastropods.

The thickness of this microfacies diminishes laterally and eventually disappears (Fig. 18e-h).

Interpretation

These sediments settled in the nearshore region when the sea level dropped, forming the bioclastic grainstone facies. This microfacies is related to the gray shale facies.

4.3. Facies association in the middle to the upper part of the sections

Massive conglomerate lithofacies (Gm)

Description

This lithofacies can be observed in the upper sections of the Aghajari Formation within the Afrineh syncline (Fig. 19a). The thickness of this facies varies from 0.5 to 4.5 m. It presents as a conglomerate with a matrix, typically displaying massive characteristics, though it occasionally shows faint layering. The constituent clasts range from subangular to subrounded, with some exhibiting significant rounding (Fig. 19b). The lower boundary of this facies is abrupt and erosional, whereas the upper boundary may be abrupt or gradual. It generally consists of a massive, matrix-supported conglomerate with a matrix of medium to coarse sandstone or gravels (2-4 mm) primarily comprising siliceous material (chert), filling the space between clasts. Clasts are mostly

sub-angular to sub-rounded, fine to coarse pebbles, but cobble-sized clasts also occur in the lower parts.

Interpretation

According to Harms et al. (1982), this lithofacies results from strong currents, which relate to the occurrence of a fine-grained matrix during waning flow. The poor sorting of the clasts, the large quantity of grains, and the massive structure suggest the presence of powerful currents (Ghazai and Mountney, 2009). The absence of cross-stratification is attributed to a lower ratio of water depth to average particle size (Rust, 1978). According to Costa (1988) and Shanmugam (1996), the massive structure, poor sorting, and sandy matrix indicate deposition resulting from non-cohesive granular flow. Simpson et al. (2002) related facies Gm to highly concentrated flows. The considerable volume of sediment is essential for forming this facies (Kumar et al., 2003, 2007). The Gm reflects longitudinal bars in braided rivers, gravelly sheets, and channel deposits (Williams and Rust, 1996; Hein and Walker, 1977; Reineck and Singh, 1980; Miall, 1996).

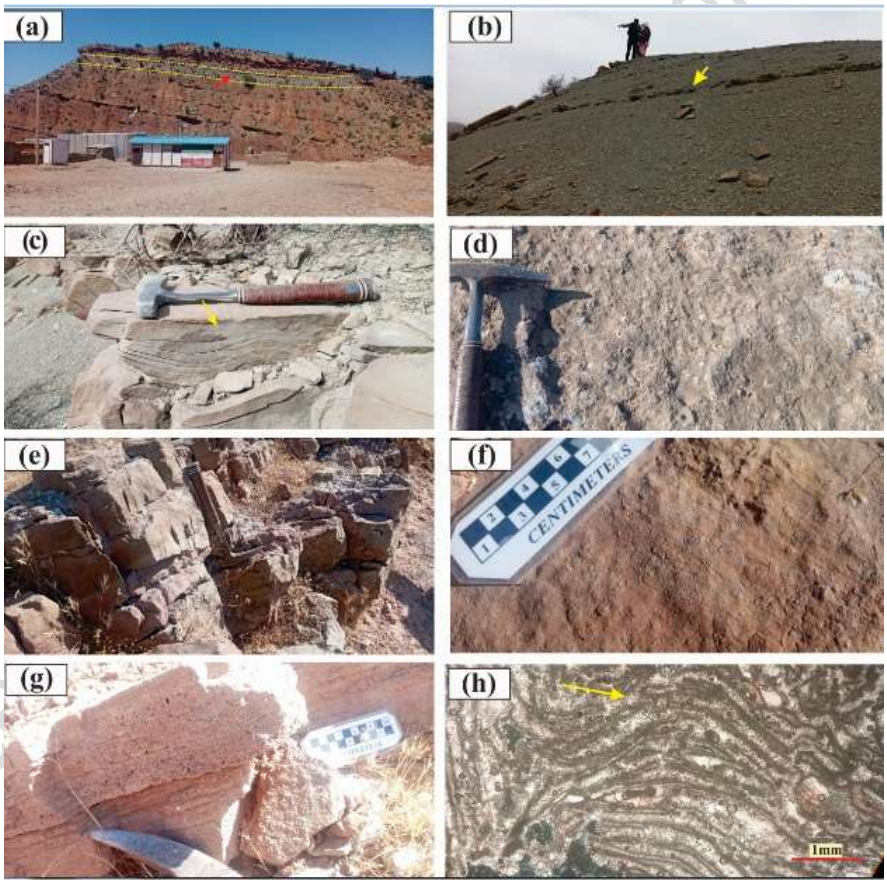

Figure 18. (a) Gray shale unit (the yellow dashed line); (b) A close-up view of (a). The yellow arrow marks the interbedded sandstone; (c) and (d) represent the sandy interbed and bioclastic grainstone facies, respectively; (e), (f), and (g) Field photographs of the bioclastic grainstone microfacies; (h) photomicrograph of the bioclastic grainstone. The fossil fragments show alignment (yellow arrows).

Planar cross-bedded conglomerate lithofacies (Gp)

Description

This grain-supported lithofacies features cross-beds inclined at angles ranging from 15 to 25 degrees. (Fig. 19-c and d). The thickness of this facies is variable from 0.5 to 2.5 m. It displays planar cross-stratification. The lower and upper boundaries of Gp are erosional. Occasionally, erosional surfaces create separations between the cross-beddings. It generally consists of normal grading, matrix to clast-supported conglomerate, characterized by a matrix of medium to coarse sand or gravel (2-4 mm) that primarily comprises siliceous material (chert) filling the space between clasts. Clasts are mostly sub-angular to sub-rounded, fine to medium to coarse pebbles, but cobble-sized clasts also occur in the lower parts.

Interpretation

Each set of Gp is less than 2.5 meters thick, forming smaller sediment bodies (Bose and Chakraborty, 1994; Chakraborty et al., 2017). The erosional surfaces form due to variations in local current velocity and sediment supply (Allen, 1983). Miall (1985) describes Gp as the migration of transverse bars in the deeper parts of a channel. Harms and Fahnestock (1965) observed that higher flow velocities lead to the deposition of coarse grains in braided rivers, while periods of lower flow velocities result in the deposition of fine-grain sediments. The occurrence of lenticular sandstones within Gp can be attributed to a reduction in the current strength (Miall, 1985).

Trough cross-bedded conglomerate lithofacies (Gt)

Description

This lithofacies is characterized by conglomerates that can be grain-supported or matrix-supported, often accompanied by trough stratification (Fig. 19-e). The thickness of this facies is variable from 0.5 to 2 m. The conglomerate found within this lithofacies exhibits moderate to poor sorting, with particle sizes ranging from granules to pebbles. It demonstrates a range of roundness and sphericity that can be classified as moderately to well-rounded. Most particles consist of siliceous material (chert) and carbonate. This lithofacies is mainly found as a set and a coset of cross-strata. The lower boundary of this facies shows good symmetry. Lithological characteristics of gravels are generally similar to those of lithofacies Gm and Gp. Typical dimensions of individual units range from 0.5-1m in thickness and usually 1-3m in lateral extent.

Interpretation.

The symmetry observed in the lower boundary implies a fast accumulation of material within the channel cutouts (Teisseyre, 1975; Yagishita, 1997). A single set in Gt suggests that the filling occurred in one stage (Ramos and Sopena, 1983). This facies is formed through channel infilling (Miall, 1977). However, some researchers related it to migrating three-dimensional gravel bars in braided rivers (Bridge and Mackey, 1993; Browne and Plint, 1994).

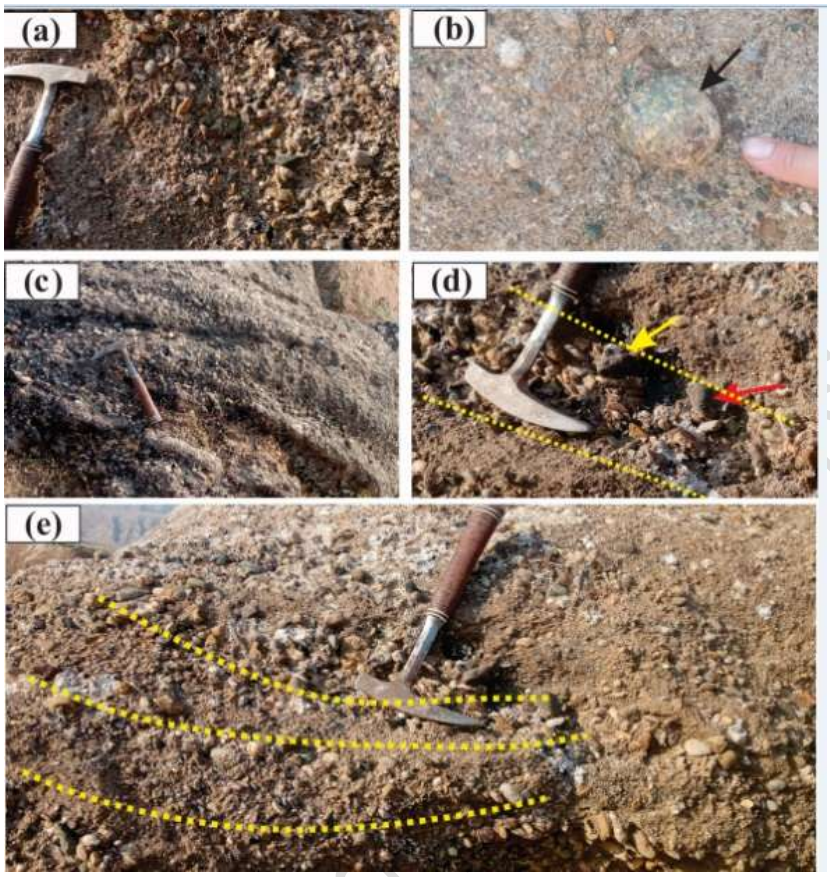

Figure 19. (a) Lithofacies Gm with abundant pebble-sized clasts; (b) Lithofacies Gm with abundant granule-sized clasts. The black arrow indicates the well-rounded cherty gravel; (c) A two-set cross-stratification in Gp; (d) Lithofacies Gp showing normal grading; (e) Lithofacies Gt.

Sandstone facies with trough cross-stratification (St)

Description

This facies can be found in all parts of the sequences within environments like meandering rivers, shallow marine coastlines, and braided river systems. The primary distinction between facies St in braided rivers and those in meandering rivers lies in the scale of the sedimentary structures (Fig. 20), particle size, and color variations. Facies St in braided rivers exhibits significantly larger dimensions, coarser grains, a gray color, and high lateral extension. In contrast, in meandering rivers and the shallow sea (the lower sections of the investigated sequence), facies St is typically smaller, features finer grains, and exhibits a brown to red color. These sandstones are submature and consist of chertarenite and calclitharenite petrofacies.

Interpretation

Unimodal orientation of trough cross-beds is favorable in a fluvial bed system (Eriksson et al., 1998; Miall, 1996). Trough cross-bedded sandstone is interpreted as the product of 3-D dunes

migrating in channels under the upper part of the lower flow regime or infilling of scour hollows (Collinson and Thompson, 1992; Harms et al., 1982; Miall, 1977)

Horizontally stratified sandstone facies (Sh)

Description

This lithofacies is prevalent throughout the entire sequences, particularly in the upper parts. The main features include significantly thick sandstone units (exceeding 6 meters) that extend laterally over large areas, as well as parting lineation (see Fig. 20c, d, e). The associated sediments vary from medium to coarse sand and demonstrate poor to moderate degrees of roundness and sorting. The main elements of their petrofacies consist of chertarenite and calclitharenite.

Interpretation

Facies Sh typically develops in braided river settings characterized by upper flow regimes, as noted by Boothroyd and Ashley (1975), Harms et al. (1982), Allen (1984), Miall (1996), Jo et al. (1997), and Lee and Chough (2006).

Massive sandstone facies (Sm)

Description

The facies Sm is characterized by a substantial thickness ranging from 2 to 6 meters, a predominance of coarse-grained sand particles, and a limited lateral extent (Fig. 20-f). It occurs as sand bars situated within the channels of braided river systems. These sandstones are submature and consist of calclitharenite petrofacies.

Interpretation

Sm facies, alongside lenticular mudstones and conglomerate facies, provide evidence for associating this lithofacies with braided river environments (Harms et al., 1982; Reading, 1996; Miall, 1996).

Fine-grained lithofacies

The fine-grained lithofacies can be found in the lower parts of all investigated areas. These particular lithofacies primarily develop as overbank deposits in meandering river systems. In contrast, the mudstones form distinct lens shapes within braided river deposits with limited lateral extension (Fig. 20 g and h). These muddy lenses are characteristic of low-energy settings between sandy and gravelly bars.

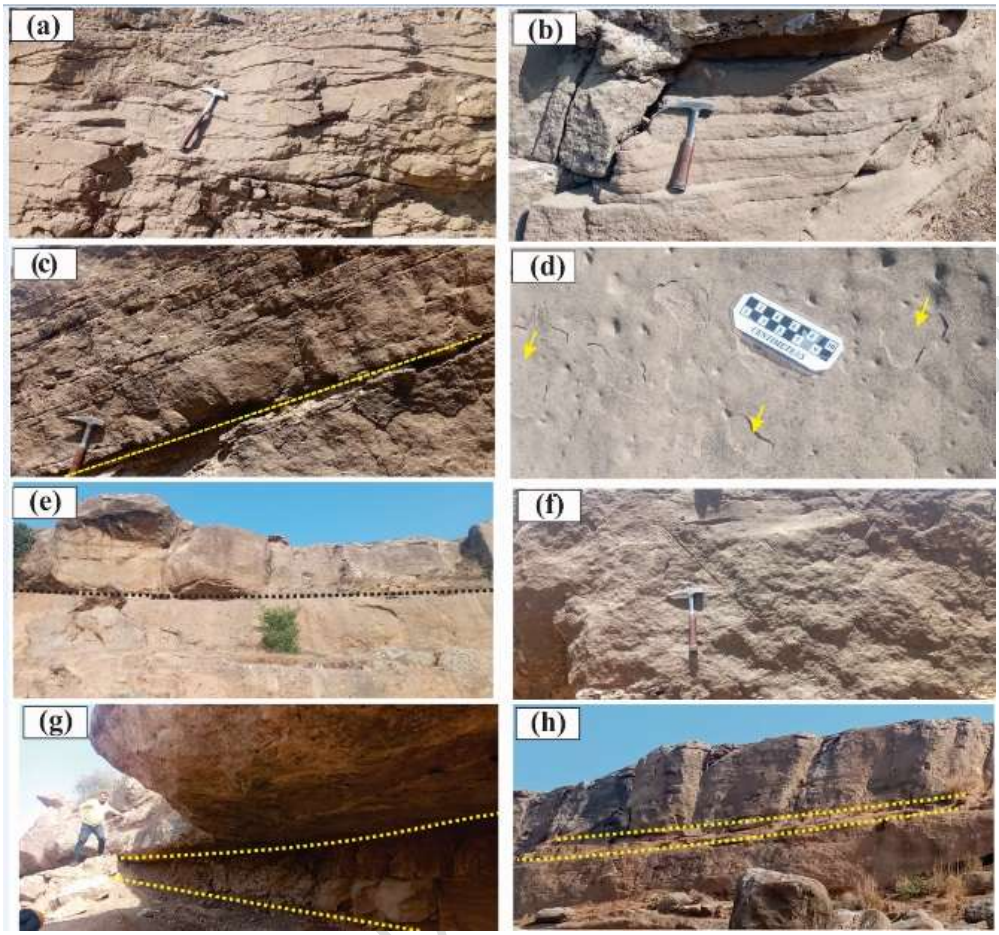

Figure 20. (a) and (b) Large-scale trough bedding in sandy deposits of braided river systems; (c), (d) and (e) the Sh lithofacies in braided river systems. It is featured by significant thickness and parting lineation (yellow arrows in b); (f) Massive sandstone lithofacies; (g) and (h) Limited extension of lens-shaped fine-grained facies (within the yellow dashed lines) in braided rivers.

5. Discussion

Depositional model for the Aghajari Formation (Afrineh syncline)

Field observations and lithofacies analysis indicate that the lower parts of the Aghajari Formation, which lie over the Gachsaran Formation, originated in a meandering river environment. Following a marine transgression, these meandering river deposits were subsequently overlain by tidal flat sediments, which were later buried under both deep and shallow marine deposits. As a result, these sequences underwent a marine regression, leading to the deposition of meandering and braided river sediments on top of them.

The Aghajari Formation begins with the emergence of the initial facies, characterized by red mudstone and sandstone. Three significant structural elements were genetically classified based on facies associations, geometry, sedimentary structures, and lithology within the Aghajari

Formation. These elements consist of channel (CH), crevasse splay (CR), and floodplain (OF). The lower part of the Aghajari Formation features sandstone facies (St, Sp, and Sh), concave-upward erosion surfaces, single-story channels, and a lenticular shape, with thicknesses reaching up to 5 meters and widths varying from 7 to 15 meters.

The structural component CR was recognized in this section. Crevasse splays primarily exhibit lenticular or wedge-shaped forms and have thicknesses ranging from 0.1 to 0.6 m, gradually reducing their lateral extent (Fig. 21). The fine-grained sandstone or siltstone (facies Sh) displays horizontal lamination and is surrounded by reddish-brown mudstone deposits (Fm) is interpreted as crevasse splay complexes created by overtopped channel levees during flood events (Miall, 2006; Ghazi and Mountney, 2009; Teng et al., 2024). In this research, the overbank flow structural element (OF), which is quite prevalent, primarily consists of massive reddish-brown mudstone facies (Fm). The assemblages of overbank deposits feature both large- and small-scale lensoidal channel facies (St and Sh), which correspond to structural elements CH and CR, along with massive mudstone (Fm). The thickness of the overbank deposits exceeds 60 m. The facies assemblage contains trace fossils, including ichnofossils like Skolithos, Ophiomorpha, and Thalassinoides.

According to the evidence presented, it can be concluded that the lower part of the Aghajari Formation within the Afrineh syncline, which is adjacent to the Gachsaran Formation, consists of meandering river facies (Fig. 21):

1- The lens-shaped channels, characterized by erosional bases and restricted lateral extent, have cut the floodplain mudstones.

2- The mudstone and siltstone facies, characterized by their sheet-like shape and broad lateral extent, suggest that they were formed in an overbank setting.

3- The sandstone facies related to the crevasse splay had a wedge-like shape due to river levees being breached during floods, leading to sediment deposition on the floodplain.

4- There are multiple sand and shale cycles, transitioning from sand to shale upwards.

5- Abundant trace fossils in the facies.

6- Sandstones with poor textural and compositional maturities indicate a fluvial setting (Gingras et al., 2011).

Therefore, it can be inferred that the sequences of the Aghajari Formation in the Afrineh Syncline were developed in four distinct depositional environments: meandering rivers, tidal flats, deep and shallow marine environments, and meandering and braided rivers (Fig. 22).

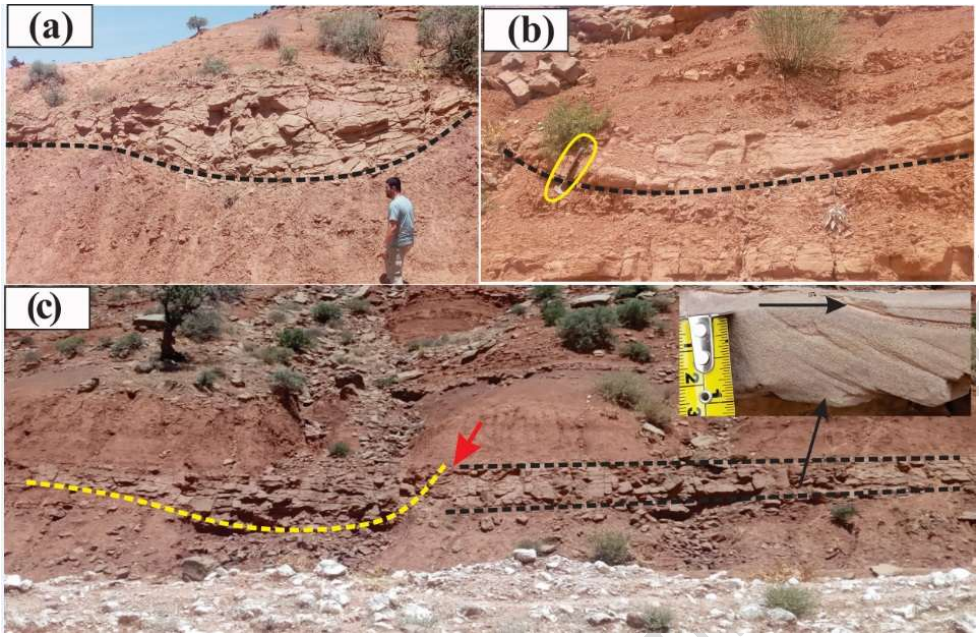

Figure 21. (a) A meandering river channel cut the fine-grained deposits. (b) A smaller-sized meandering river channel. The middle part of the studied sequences. (c) A meandering river channel and crevasse splay (The red arrow indicates the boundary between two subenvironments).

The sandstone lithofacies found in shallow marine coastal regions influenced by tidal activity typically show moderate to good sorting. This environment features sedimentary structures, including flaser bedding, interference ripple marks, symmetrical ripple marks, and reactivated surfaces (Figs. 12-14). Furthermore, the Skolithos trace fossil is found in facies associated with shallow, sandy coastal settings. Considering its connection to flaser and wave-dominated strata, it can be inferred that these relate to intertidal sandy shorelines (Dashtgard et al., 2010; Chakraborty et al., 2017). The trace fossils discovered in this environment are Lockeia, Planolites, irregular Ophiomorphs, Paleophycus, and Taenidium (Fig. 15). These trace fossils are closely related to the Skolithos trace fossil, associated with intertidal sandy shorelines (Seilacher, 1967 and 2006; Aguirre et al., 2010; Sharafi et al., 2012).

In all sections, a gray shale layer rich in planktonic fauna has been identified, indicating the presence of a key bed. The thickness of this layer varies between 2 and 10 meters (see Figs. 16-18). Another lithofacies in the marine environment is the bioclastic grainstone facies, which forms in shallower areas. These marine deposits overlay the meandering river facies and are primarily found in the central part of the Aghajari Formation. The thickness of this microfacies ranges from a few centimeters up to a maximum of 1.5 meters, gradually thinning laterally until it disappears. The bioclastic grainstone comprises 80 to 90 percent bivalve skeletal remains and small gastropods exceeding 2 millimeters. Calcite cement fills the pore spaces between skeletal grains (see Figs. 18e-h).

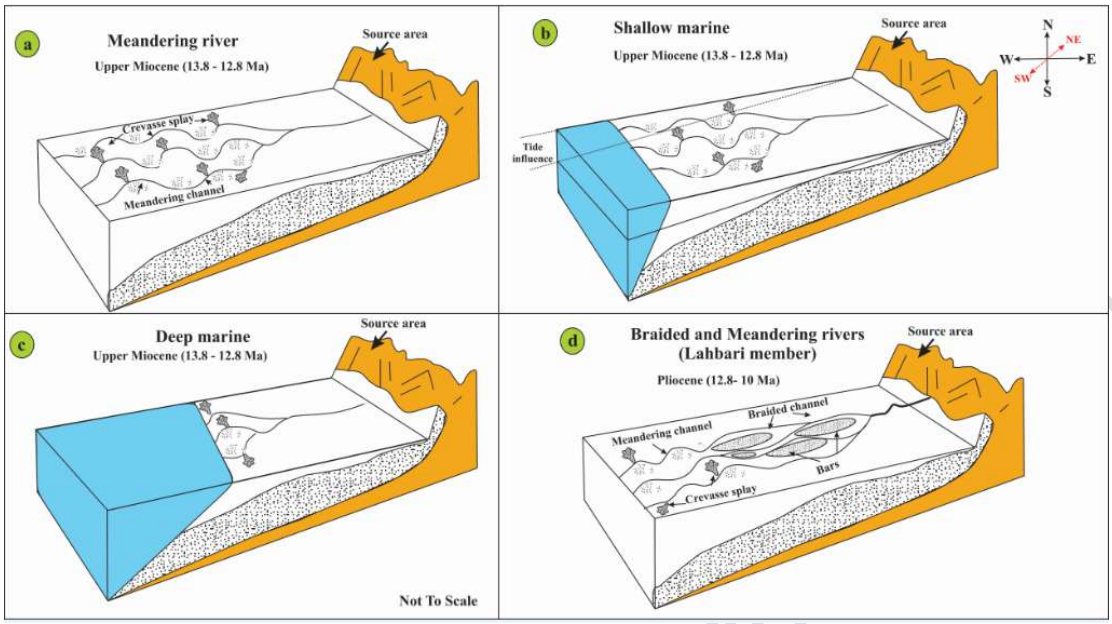

Figure 22. Changes in the depositional environment of the Aghajari Formation in the Afrineh syncline were caused by the transgression and regression of seawater. These changes occurred in four stages: a) the expansion of the meandering river facies. b) the beginning of the rise of sea level and the formation of the facies of the shallow tidal part. c) The vast advance of the sea level and the formation of shales in the deep part of the sea. d) the falling sea level and the formation of the braided and meandering river facies.

The Lahbari member covers the marine sediments, suggesting a falling sea level (Fig. 22-d). The lower part of the Lahbari member comprises deposits from meandering rivers that gradually transition into a braided river setting in the upper parts. One of the significant features of braided river deposits is the presence of conglomerate facies alongside sandstone bodies that appear in sheets and lenses, as well as mudstones that show limited lateral extents (Figs. 19 and 20). The Lehbari Member is distinct from the middle and lower sections of the Aghajari Formation in terms of particle size, sedimentary structure dimensions, and coloration. The Lehbari member contains coarser particles, and its sedimentary structures are of greater scale. This member displays a color range from gray to cream. The depositional settings of the Aghajari Formation within the Afrineh syncline, from the base to the top of the sections, consist of meandering rivers, tidal flats, marine environments, and meandering and braided river systems. Global sea level changes, resulting from tectonic activities or climate changes, can explain these shifts. The transgression and regression of seawater have led to changes in the depositional settings. A meandering river environment developed on the Gachsaran Formation at the first stage (see Fig. 22a). As sea levels rose, a tidal sandy shore was deposited (see Fig. 22b), and a deeper marine shale bed was laid down (see Fig. 22c). Later, as sea levels fell, shallow marine sediments accumulated, succeeded by meandering and braided river facies atop the sequences (Fig. 23).

The findings of this study align with global sea level fluctuation charts (Haq et al., 1987; Torfstein and Steinberg, 2020; Sosdian et al., 2020), global oxygen isotope variations during the Miocene-

Pliocene period (Lewis et al., 2014), and, based on the Nd isotope record (Bialik et al., 2019), suggest that the fall in sea levels commenced in the early Miocene (Langhian stage). Significant global glaciation was observed during this period, which may have been the primary cause of the worldwide sea level fall. This global decrease has also been documented in other regions (Passchier et al., 2013; Griener et al., 2015; Bassant et al., 2017; Raitzsch et al., 2021). The Miocene sedimentary basin in Iran was linked to other oceans (Reuter et al., 2009), and this worldwide sea level fall influenced the deposits in Iran, resulting in the formation of continental facies, such as a meandering river system. At the end of the Middle Miocene, a rapid rise in sea level occurred due to the melting of glaciers, resulting in the development of marine facies. Subsequently, during the upper Miocene, the sea retreated, leaving behind continental facies.

The study in the region is based on recognizing and interpreting lithofacies and structural elements, followed by recognizing different depositional environments along the sections studied. These depositional environment changes are caused by the marine transgression and regression that occurred in the study area during the Miocene/Pliocene period. These results are consistent with those of Sun et al. (2021) in the study area. Sun et al. (2021) investigated the sedimentary sequences of the Aghajari and Gachsaran formations within the Afrineh syncline through magnetic stratigraphy. This research yielded several key findings, including the following points:

1- Four sedimentary sequences (S1, S2, S3, S4) have been recognized within the Afrineh syncline. The sequences S1 (from 17 to 15 million years) and S2 (from 15 to 13.8 million years) are associated with the Gachsaran Formation, whereas sequences S3 (from 13.8 to 12.8 million years) and S4 (from 12.8 to 10 million years) are related to the Aghajari Formation.

2- The age of the boundary separating the Gachsaran and Aghajari formations was determined to be 13.8 million years based on magnetic stratigraphy.

3- The top of the deep marine shale bed was established 12.8 million years ago. Consequently, the lower part of the Aghajari Formation was deposited over approximately one million years.

4- The sedimentation rate in the lower part of the Aghajari Formation (Afrineh syncline) is 218 meters per million years; thus, changes in global climate have exerted the most significant impact on the sedimentation cycles in this lower part, while tectonics played the most negligible role.

5- The top of the gray marine shale bed, aged 12.8 million years, was identified as the maximum flooding surface.

6- The sequences of the Gachsaran Formation (sequences 1 and 2) indicate shallow marine conditions found primarily in lagoon and sabkha settings. Between the lower boundary of the Aghajari Formation and the marine shale bed (sequence 3), the facies demonstrate variations between marine and continental settings. From the top of the marine shale bed to the top of the sequences (sequence 4), continental deposits formed due to the expansion of Antarctic glaciers (sea regression) and the effects of regional tectonics.

7- The upper part of the Gachsaran Formation and the lower part of the Aghajari Formation (sequences 2 and 3) are affected by mid-Miocene climatic changes over 2.2 million years.

8- The boundary between the Aghajari and Gachsaran formations (aged 13.8 million years) coincides with the expansion of the East Antarctic ice sheets (Antarctica).

In the study area, the lower sequences of the Aghajari Formation, which are adjacent to the Gachsaran Formation, were formed in a meandering river setting. As a result of marine transgression, these sediments lie underneath the sediments of tidal flats and marine deposits. The melting of the Antarctic ice sheets has a global impact on these changes. As a result, these sequences encountered a regression, leading to the deposition of meandering and braided river facies above them. From the highest point of the marine shale, seen as the maximum flooding surface, to the top of the sequences, the region is more influenced by local tectonic activities. The stratigraphic architecture of alluvial successions can be controlled by three allogenic processes, including sea level changes, climate, and tectonics (Alonso-Zarza et al., 2012; Allen et al., 2013b).

Meandering rivers develop in areas with more stable tectonic activity and gentle gradients, whereas braided rivers emerge in regions with steeper slopes and more significant tectonic activity. The shift from the meandering river to braided river deposits at the upper part suggests the impact of increasing tectonic activities in the region (Burke et al., 1990; Catuneanu and Elango, 2001; Catuneanu, 2003; Vandenberghe et al., 2003; Miall, 2010; Alonso et al., 2012; Allen et al., 2013a).

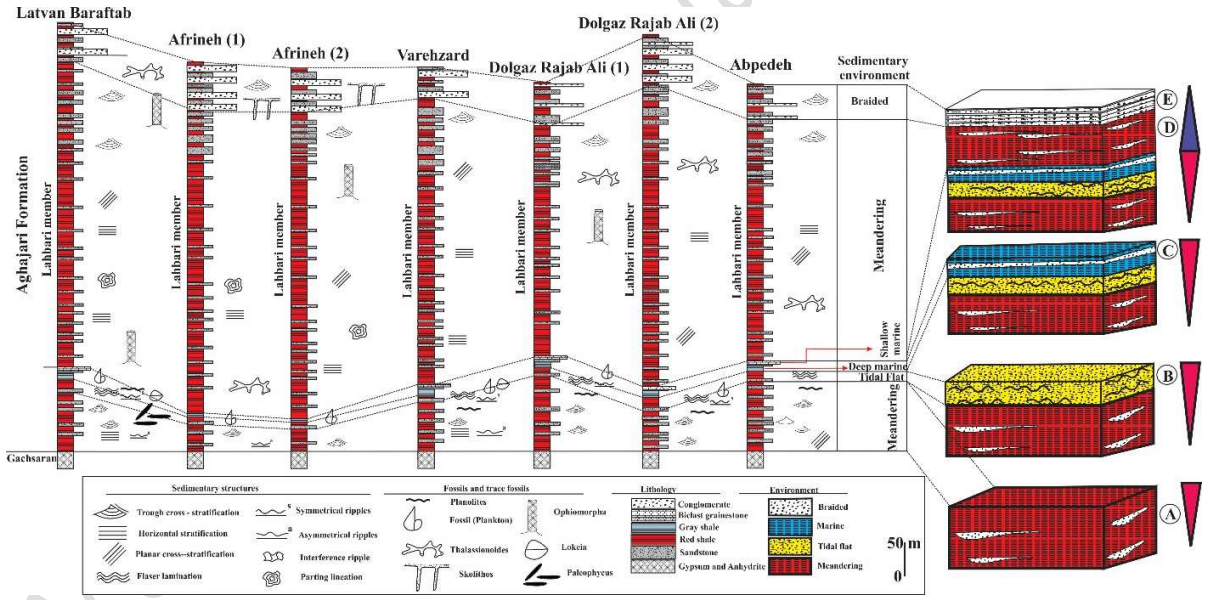

Figure 23. This stratigraphic column illustrates the sections of the Aghajari Formation located in the Afrineh syncline, accompanied by the depositional model (not to scale). A. Represents a meandering river environment, marking the base of the sequences; B. Indicates the onset of marine transgression, leading to the development of tidal flat facies; C. Shows ongoing marine transgression and submergence, which results in the formation of deep marine shale facies and bioclastic grainstone within a shallow marine setting; D. depicts marine regression resulting in the creation of meandering river facies; E. Illustrates the expansion of braided river facies.

6. Conclusion

Field investigations conducted on seven stratigraphic sections of the Aghajari Formation located in the southwest region of Khorramabad (Afrineh syncline) have resulted in the identification of three conglomerate lithofacies (Gm, Gp, Gt), nine sandstone lithofacies (Sp, St, Sm, Sh, Sr, Sfl, Sl, Slr, Sr(Fl)), four mudstone lithofacies (Fm, Fl, Fcf, Fl(sr)), one gray shale facies rich in planktonic fauna, and one bioclastic grainstone facies. A trace fossil of Skolithos, commonly found in association with sandy shorelines, was discovered within these layers. The lower part of the Aghajari Formation, situated above the Gachsaran Formation, was formed in a meandering river environment. Following marine transgression, these sediments are covered by tidal flat deposits and gray shale, indicative of a deep marine environment and bioclastic grainstone facies associated with a shallow marine setting.

The melting of Antarctic glaciers has led to changes in depositional environments. As a result, a marine regression allowed for the deposition of meandering and braided river facies, which are part of the Lahbari Member. This member formed due to a drop in global sea levels and the effects of regional tectonics.

The sequences found in the Aghajari Formation within the Afrineh syncline appear to have developed in various sub-environments, including meandering rivers, tidal flats, deep marine environments, shallow marine environments, and meandering and braided river systems. The changes in depositional environments in the lower parts of the Aghajari Formation, comprising meandering rivers, tidal flats, deep marine, and shallow marine environments, are driven mainly by global sea level fluctuations. In contrast, the Lahbari Member, which represents the upper parts of the Aghajari Formation (characterized by meandering and braided river environments), is primarily influenced by regional tectonic changes.

7. Acknowledgments

Bu-Ali Sina University of Hamedan financially supported this research. Special thanks to Professor Dr. Nasrollah Abbasi for identifying the trace fossils. We are also grateful to the anonymous reviewers for their insightful suggestions.

References

Agard P., Omrani J., Jolivet L., Whitechurch H., Vrielynck B., Spakman W., Moni´e P., Meyer B., Wortel R. (2011) Zagros orogeny: a subduction-dominated process. *Geological Magazine.* 148, 692–725. DOI:https://doi.org/ 10.1017/S001675681100046x

Aguirre J., Gibert JM., Bernabeu A.P. (2010) Proximal-distal ichnofabric changes in a siliciclastic shelf, Early Pliocene, Guadalquivir Basin, southwest Spain. *Palaeogeography, Palaeoclimatology, Palaeoecology* 291: 328–337. DOI: https://doi.org/10.1016/j.palaeo.2010.03.004

Aigbadon G. O., Akakuru O. C., Akudo E. O. (2023) Facies, textural and geochemical evaluation of the post-Santonian sandstones in the Bida basin, Nigeria: implications for control on hydrocarbon sandstone reservoir characteristics and paleoenvironments, *Unconventional Resources*. 3, 192–211. DOI: https://doi.org/10.1016/j.uncres.2023.03.004

Alavi M. (2004) Regional Stratigraphy of the Zagros Fold-Thrust Belt of Iran and Its Proforeland Evolution. *American Journal of Science*, 304: 1-20. DOI:https://doi.org/ 10.2475/ajs.304.1.1

Alavi M. (1994) Tectonics of the Zagros Orogenic Belt of Iran: *New Data and Interpretation. Tectonophys*. 229, 211–238. DOI:https://doi.org/10.1016/0040-1951(94)90030-2.

Allen, J.R.L. (1964). Studies in fluviatile sedimentation: Six cyclothems from the Lower Old Red Sandstone, Anglo-Welsh Basin. *Sedimentology* 3, 163-198. DOI: https://doi.org/10.1111/j.1365-3091.1964.tb00459.x

Allen J.R.L. (1983) Studies in fluvial sedimentation: bars, bar complexes and sandstone sheets (low-sinuosity braided streams) in the Brownstones (L. Devonian), Welsh Borders. *Sedimentary Geology*, 33, 237- 293. DOI: https://doi.org/10.1016/0037-0738(83)90076-3

Allen J.R.L. (1984) "Sedimentary structures: their character and physical basis, in developments in sedimentology," *Amsterdam: Elsevier*, 663 pp.

Allen J.P., Fielding C.R., Gibling M.R., Rygel M.C. (2013a) Recognizing products of palaeoclimate fluctuation in the fluvial stratigraphic record: an example from the Pennsylvanian to Lower Permian of Cape Breton Island. *Sedimentology* 51(5):1332–1381. DOI: https://doi.org/10.1111/j.1365-3091.2013.12102.x

Allen J.P., Fielding C.R., Rygel M.C., Gibling M.R. (2013b) Deconvolving signals of tectonic and climatic controls from continental basins: an example from the late Paleozoic Cumberland Basin, Atlantic Canada. *Journal Of Sedimentary Research* 83:847–872. DOI: https://doi.org/10.2110/jsr.2013.58

Alonso-Zarza A.M., Meléndez A., Martín-García R., Herrero M.J., Martín-Pérez A. (2012) Discriminating between tectonism and climate signatures in palustrine deposits: lessons from the Miocene of the Teruel Graben, NE Spain. *Earth Science Reviews* 113:141–160. DOI: https://doi.org/10.1016/j.earscirev.2012.03.011

Amiri-Bakhtiar H., Nouraee-Nezhad M.R. (2022) Stratigraphy of Zagros. *Publication of the oil-rich area in the south*. 390 pp. (In Persian)

Bahrami M. (2009) Lithofacies and sedimentary environments of Aghajari Formation in Dehsheikh Mountain, west of Shiraz, Iran. *World Applied Sciences Journal*, 6(4): 464-473.

Bahroudi A., Koyi H.A. (2004) Tectono-sedimentary framework of the Gachsaran Formation in the Zagros foreland basin. *Marine and Petroleum Geology*. 21, 1295–1310. DOI: http://doi.org/10.1016/j.marpetgeo.2004.09.001

Bassant P., Janson X., van Buchem F., Gurbuz K., and Eriş. K. (2017) Mut Basin, Turkey: Miocene carbonate depositional styles and mixed systems in an icehouse setting. *American Association of Petroleum Geologists Bulletin*. DOI: https://doi.org/101(4): 533-541.Doi:10.1306/011817DIG17032.

Bhattacharyya A., Chakraborty C. (2000) Analysis of Sedimentary Successions, A Field Manual, A.A. *Balkema Publishers*, 408p. DOI: https://doi.org/10.1017/S0016756801335598

Bialik O.M., Frank M., Betzler C., Zammit R., Waldmann N.D. (2019) Two-step closure of the Miocene Indian Ocean Gateway to the Mediterranean. *Science Reviews. 9, 8842*. DOI: https://doi.org/10.1038/s41598-019-45308-7

Bose P.K., Chakraborty P.P. (1994) Marine to fluvial transition: Proterozoic Upper Rewa Sandstone, Maihar, India. *Sedimentary Geology*, 89, 285-302. DOI: https://doi.org/10.1016/0037-0738(94)90098-1

Boothroyd J.C., Ashley G.M. (1975) "Processes, bar morphology, and sedimentary structures on braided outwash fans, northeastern Gulf of Alaska," *Society of Economic Paleontologists and Mineralogists Special Publication*, Vol. 23: 193- 222. DOI: https://doi.org/10.2110/pec.75.23.0193

Burke K., Francis P., Wells G. (1990) Importance of the geological record in understanding global change. *Paleogeography, Paleoclimatology, Paleoecology*, 89, 193-204. DOI: https://doi.org/10.1016/0921-8181(90)90016-6

Bridge J.S., Mackey S.D. (1993) A revised alluvial stratigraphy model. In: Marzo, M., Puigdefabregas, c. (eds.), Alluvial Sedimentation. *Special Publication International Association of Sedimentologists*, 17, 319-336. DOI: https://doi.org/10.1002/9781444303995.ch22

Browne G.H., Plint A.G. (1994) Alternating braidplain and lacustrine deposition in a strike-slip setting: the Pennsylvanian Boss Point Formation of the Cumberland Basin. *Journal of Sedimentary Research*, B, 64, 40-59. DOI:https://doi.org/10.1306/d4267f41-2b26-11d7-8648000102c1865d

Catuneanu O., Elango H. (2001) Tectonic control on fluvial styles: the Balfour Formation of the Karoo Basin, South Africa. *Sedimentary Geology* 140 (2001) 291±313. DOI: https://doi.org/10.1016/S0037-0738(00)00190-1

Catuneanu O. (2003) "Sequence stratigraphy of clastic systems," *Geological Association of Canada, Short Course Notes*, 248 pp. DOI: https://doi.org/10.1016/S0899-5362(02)00004-0

Chakraborty P.P., Saha S., Das K. (2017) Record of continental to marine transition from the Mesoproterozoic Ampani basin, central India: An exercise of process-based sedimentology in a structurally deformed basin; *Journal of Asian Earth Sciences*. 143 122–140. DOI: https://doi.org/10.1016/j.jseaes.2017.04.015

Collinson J.D., and Thompson D.B. (1992) Sedimentary Structures, 2nd ed. Unwin Hyman, London, 207 p. (1989). 17. Crimes, T.P. and Droser, M.L. Trace fossils and bioturbation: The other fossil record. Annu. Rev. *Scientific Research*, 23, 339-360.

Costa J.E. (1988) Rheologic, geomorphic, and sedimentologic differentiation of water floods, hyper-concentrated flows, and debris flows. In: V. R. Baker, R. C. Kochel, and P. C. Patton (eds.), *Flood Geomorphology. Wiley, New York, NY*, 113- 122.

Cushman J.A. (1926) Recent foraminifera from Porto Rico. *Publications of the Carnegie Institution of Washington*. 342: 73-84.

Dalrymple R.W., Zaitline B.A., Boyd R. (1992) Estuarine facies models: Conceptual basis and stratigraphic implications. *Sedimentary Research*. V. 62, p. 1130-1146. DOI: https://doi.org/10.1306/D4267A69-2B26-11D7-8648000102C1865D

Dashtgard S.E., MacEachern J.A., Frey S.E., Gingras M.K. (2010) Tidal effects on the shoreface: Towards a conceptual framework. *Sedimentary Geology* 279: 42-61. DOI: https://doi.org/10.1016/j.sedgeo.2010.09.006

Davis R.A. (2012) Tidal signatures and their preservation potential in stratigraphic sequences. In: Davis, R.A. and Dalrymple, R.W. (Eds.), *Principles of Tidal Sedimentology. Springer*, p. 35-55. DOI: https://doi.org/10.1007/978-94-007-0123-6_3

Dongyang C., Feng W., Hongde C. et al. (2019) Characterization of braided river reservoir architecture of the Upper Paleozoic He 8 member on Fugu Tianshengqiao outcrop, eastern Ordos Basin, *Oil Gas Geology*. 40 (2) 335–345. DOI: https://doi.org/10.11743/ogg20190212

Dunham R.J. (1962) Classification of carbonate rocks according to depositional texture. *American Association of Petroleum Geologists Bulletin*, p. 108-121.

Emami H. (2008) Foreland Propagation of Folding and Structure of the Mountain Front Flexure in the Push t-E-Kuh Arc (Zagros, Iran). *Universitat de Barcelona, Barcelona*.

Eriksson P. G., Condie K. C., Tirsgaard H., Muller W. U., Altermann W., Miall A. D., Aspler L. B., Catuneanu O., and Chiarenzelli J.R. (1998) Precambrian clastic sedimentation systems. *Sedimentary Geology*. 120, 5-53. DOI: https://doi.org/10.1016/S0037-0738(98)00026-8

Fakhari M. (1985) Khurramabad Geological Compilation Map 1/100,000 (Sheet 20813W). *National Iranian Oil Company, Tehran*.

Gani R.M., Alam M.M. (2004) "Fluvial facies architecture in small-scale river system in the Upper Dupi Tila formation, Northeast Bengal basin, Bangladesh," *Journal of Asian Earth Sciences*, Vol. 24: 225- 236. DOI: https://doi.org/10.1016/j.jseaes.2003.11.003

Gingras M.K., MacEachern J.A., Dashtgard S.E. (2011) The potential of trace fossils as tidal indicators in bays and estuaries. *Sedimentary Geology*, V. 279, p. 97-106. DOI: https://doi.org/10.1016/j.sedgeo.2011.05.007

Gill W.D., Ala M.A. (1972) Sedimentology of Gachsaran Formation (lower Fars series), Southwest Iran. *American Association of Petroleum Geologists Bulletin*. 56, 1965–1975. DOI: https://doi.org/10.1306/819A41A0-16C5-11D7-8645000102C1865D

Ghazi S., Mountney N.P. (2009) Facies and architectural element analysis of a meandering fluvial succession: The Permian Warchha Sandstone, Salt Range, Pakistan, *Sedimentary Geology*, 221,99-126. DOI: https://doi.org/10.1016/j.sedgeo.2009.08.002

Ghorbani M. (2015) Stratigraphy of Iran. *Arian Zamin Publication*. 330 pp. (In Persian)

Ghosh P., Sarkar S., Maulik P. (2006) "Sedimentology of a muddy alluvial deposit: Triassic Denwa Formation, India," *Sedimentary Geology*, Vol. 191: 3- 36. DOI: https://doi.org/10.1016/j.sedgeo.2006.01.002

Griener K.W., Warny S., Askin R., Acton G. (2015) Early to Middle Miocene vegetation history of Antarctica supports eccentricity-paced warming intervals during the Antarctic icehouse phase. *Global and Planetary Change*, 127: 67-78. DOI: https://doi.org/10.1016/j.gloplacha.2015.01.006

Gohari M. (2014) Petrography, sedimentary environments and sequence stratigraphy of Aghajari Formation in the northwest of Shiraz, Qalat section. Master's thesis, *Hormozgan University*, 137 p (in Persian)

Haq B.U., Hardenbol J.A.N., Vail P.R. (1987) Chronology of fluctuating sea levels since the Triassic. *Research Company, Houston*, 235(4793): 1156-1167. Lewis A. R. Marchant D. R. Ashworth A. C. DOI: https://doi.org/10.1126/science.235.4793.1156

Harms J.C., Fahnestock R.K. (1965) Stratification, bedforms, and flow phenomena (with an example from the Rio Grande). In Primary sedimentary structures and their hydrodynamic interpretation (ed. Middleton, G.V.), *Society of Economic Paleontologists and Mineralogists, Special Publication*, 12, 84-115. DOI: https://doi.org/10.2110/pec.65.08.0084

Harms J.C., Southard J.B., Walker R.G. (1982) Structures and Sequence in Clastic Rock. *Society of Economic Paleontologists and Mineralogists*, Short Course, Chapter 1, p. 55. DOI:https://doi.org/10.2110/scn.82.09

Hein F.J., Walker R.G. (1977) Bar evolution and development of stratification in the gravelly, braided, Kicking Horse River, British Columbia. *Canadian Journal of Earth Science*, 14, 562-570. DOI: https://doi.org/10.1139/e77-058

Higgs K.E., King P.R., Raine J.I., Sykes R., Browne G.H., Crouch E., Baur J.R. (2012) Sequence stratigraphy and controls on reservoir sandstone distribution in an Eocene marginal marine-coastal plain Fairway, Taranaki Basin, New Zealand. *Marine and Petroleum Geology*, V. 30, p. 175-192. DOI: https://doi.org/10.1016/j.marpetgeo.2011.12.001

James G.A., Wynd J.G. (1965) Stratigraphic nomenclature of Iranian oil consortium agreement Area, *American Association of Petroleum Geologists Bulletin*, 49: 2182-2245. DOI: https://doi.org/10.1306/A663388A-16C0-11D7-8645000102C1865D

Jones R.W., Racey A. (1994) Cenozoic stratigraphy of the Arabian Peninsula and Gulf. In: Simmons, M.D. (Ed.), Micropaleontology and Hydrocarbon Exploration in the Middle East. *Chapman and Hall, London*, pp. 273–303.

Jo H.R., Rhee C.W., Chough S.K. (1997) "Distinctive characteristics of a streamflow-dominated alluvial fan deposit; Sanghori area, Kyongsang Basin (Early Cretaceous), southeastern Korea," *Sedimentary Geology*, Vol. 110 (1-2): 51- 79. DOI: https://doi.org/10.1016/S0037-0738(96)00083-8

Kumar R., Ghosh S.K., Mazari R.K., Sangode S.J. (2003) Tectonic impact on the fluvial deposits of Plio-Pleiostocene Himalayan foreland basin, India, *Sedimentary Geology*, 158, 209-234. DOI:https://doi.org/10.1016/S0037-0738(02)00267-1

Kumar R., Suresh N., Satish J., Sangode J., Kumaravel V. (2007) Evolution of the Quaternary alluvial fan system in the Himalayan foreland basin implications for tectonic and climate decoupling. *Quaternary International*, V. 159, p. 6-20. DOI: https://doi.org/10.1016/j.quaint.2006.08.010

Lewis A.R., Marchant D.R., Ashworth A.C., Hemming S.R., Machlus M.L. (2014) Major Middle Miocene global climate change: Evidence from east Antarctica and the Transantarctic Mountains. *Geological Society of America Bulletin*. 119(11-12): 1449-1461.

Lee H.S., Chough S.K. (2006) Lithostratigraphy and depositional environments of the Pyeongan Supergroup (Carboniferous–Permian) in the Taebaek area, mid-east Korea. *Asian Earth Sciences*, V. 26, p. 339–352. DOI:https://doi.org/10.1016/j.jseaes.2005.05.003

Longhitano S.G., Mellere D., Steel R.J., Ainsworth R.B. (2012) Tidal depositional systems in the rock record: A review and new insights. *Sedimentary Geology*, V. 279, pp. 2-22. DOI:https://doi.org/10.1016/j.sedgeo.2012.03.024

Miall A.D. (1977) A review of the braided river depositional environment. *Earth Science Reviews*. Rev., 13: 1-62. DOI:https://doi.org/10.1016/0012-8252(77)90055-1

Miall A.D. (1985) Architectural-element analysis: a new method of facies analysis applied to fluvial deposits. *Earth Science Reviews*, 22: 261- 308. DOI:https://doi.org/10.1016/0012-8252(85)90001-7

Miall A.D. (1992) Collision-related foreland basin. In: Ingersol RV, Busby CJ. (Eds.), *Tectonics of Sedimentary Basin. Black Science, Oxford*, 393- 424.

Miall A.D. (1996) The Geology of Fluvial Deposits: Sedimentary Facies, Basin Analysis and Petroleum Geology. *Springer-Verlag Inc., Heidelberg*, 582 p.

Miall A.D. (2000) Principles of Sedimentary Basin Analysis. *Springer-Verlag, New York*, p. 668. DOI:10.1007/978-3-662-03999-1_7

Miall A.D. (2006) The Geology of Fluvial Deposits (3rd edition). *Springer-Verlag, Berlin*, p. 582.

Miall A.D. (2010) Alluvial deposits. In: James NP, Dalrymple RW (eds) Facies models 4, 4th ed, *Geology Association Canada*. DOI : 10.14456/sjst-psu.2021.190 pp. 105–137

Moradi B. (2014) Lithofacies, sedimentation conditions and diagenetic characteristics of Aghajari Formation in West Bandar Abbas, (Soro section). Master's thesis, *Hormozgan University*, 113 p (in Persian)

Motiei H. (1995) Geology of Iran, Stratigraphy of Zagros, *Publications of the Country Geological Organization*, 630 p (in Persian)

Motiei H. (2012) Stratigraphy of Zagros, *Publications of the Geological Organization of the Country*, 422 p (in Persian)

Orbigny A. D. d'. (1839) Foraminifères, in de la Sagra R., Histoire physique, politique et naturelle de l'ile de Cuba. *A. Bertrand.* 1-224. DOI:https://books.google.pt/books?id=KpVeAAAAcAAJ&pg

Passchier S., Bohaty S.M., Jiménez-Espejo F., Pross J., Röhl U., van de Flierdt T., Brinkhuis H. (2013) Early Eocene to Middle Miocene cooling and aridification of east Antarctica. *Geochemistry, Geophysics, Geosystems*. 14(5): 1399-1410. DOI:https://doi.org/10.1002/ggge.20106

Pettijohn C.K. (1975) Sedimentary Rocks (New York: Harper & Row), 2nd Edition, *Harper and Row Publishers, New York*, 628 p.

Pirouz M., Simpson G., Chiaradia M. (2015) Constraint on foreland basin migration in the Zagros mountain belt using Sr isotope stratigraphy. *Basin Research*. 27, 714–728. DOI:https://doi.org/10.1111/bre.12097

Powell M., Ockelford A.P., Rice S.K., Hillier J., Nguyen T., Reid I.J., Tate N, Ackerley D. (2016) Structural properties of mobile armors formed at different flow strengths in gravel-bed rivers. *Journal of Geophysical Research Earth Surface*. 121: 1494-1515 DOI:https://doi.org/10.1002/2015JF003794

Ramos A., Sopena A. (1983) Gravel bars in low sinuosity streams (Permian and Triassic, Central Spain). In: Collinson, J. D., Lewin, J. (eds.), Modern and Ancient Fluvial Systems. *Special Publication International Association of Sedimentologists*, 6, 301-312. DOI:https://doi.org/0141-3600/83/0106-0301 $02.00

Raitzsch M., Bijma J., Bickert T., Schulz M., Holbourn A., Kučera M. (2021) Atmospheric carbon dioxide variations across the Middle Miocene climate transition. *Climate of the Past*. 17(2): 703-719. DOI:https://doi.org/10.5194/cp-17-703-2021

Reading H.G. (1996) Sedimentary environments and facies: *Blackwell Scientific Publication*s, 425 p.

Reineck H.E., and Singh I.B. (1980) Depositional sedimentary environments (with reference to terrigenous clastics). 2nd. Ed., *Springer-Verlag*, 549 p.

Reuter M., Piller W.E., Harzhauser M., Mandic O., Berning B., Rögl F., Hamedani A. (2009) The Oligo-/Miocene Qom Formation (Iran): Evidence for an Early Burdigalian restriction of the Tethyan Seaway and closure of its Iranian gateways. *International Journal of Earth Sciences*. 98(3): 627-650.DOI: https://doi.org/10.1007/s00531-007-0269-9

Rust B.R. (1978) Depositional models for braided alluvium. In: Miall, A. D. (ed.), *Fluvial sedimentology*. *Canadian Society of Petroleum Geologists Memoir*, 5, 605-626.

Sahraeyan M., Bahrami M., Hejazi S.H. (2012) Identifying the sedimentary environments of the Aghajari Formation based on lithofacies and architectural elements in the southeastern Sarvestan, Fars Province. *Journal of Geotechnical Geology*, v(8)1, pp, 18-38 (in Persian)

Sakhavati B., Yousefirad M., Majidifard M.R., Solgi A., Maleki Z. (2020) Age of the Gachsaran Formation and equivalent formations in the Middle East based on Foraminifera. *Micropaleontology* 66, 441–465.

Seilacher A. (1967) Bathymetry of trace fossils. *Marine Geology*, **v.** 5, p. 413–428. DOI:https://doi.org/10.1016/0025-3227(67)90051-5

Seilacher A. (2006) Trace Fossil Analysis, *Springer*, 225p.

Selley R.C. (2000) Applied sedimentology. *Academic Press*, Second edition.

Simpson E.L., Dilliard K.A., Rowell B.F., Higgins D. (2002) The fluvial-to-marine transition within the post-rift Lower Cambrian Hardyston Formation, Eastern Pennsylvania, USA. *Sedimentary Geology*, 147-127-141. DOI:https://doi.org/10.1016/S0037-0738(01)00193-2

Shanmugam G. (1996) High-density turbidity currents: Are they sandy debris flow? *Journal of Sedimentary Research*, 66, 2-10. DOI:https://doi.org/10.1306/D426828E2B26-11D7-8648000102C1865D

Sharafi M., Ashori M., Mahboubi A., Moussavi-Harami S.R. (2012) Stratigraphy application of Thalassinoides ichnofabric in delineating sequence stratigraphic surface (Mid-Cretaceous), Kopet-Dagh Basin, northeastern Iran. *Palaeoworld*, V. 21, p. 202-216. DOI:https://doi.org/10.1016/j.palwor.2012.06.001

Sosdian S.M., Babila T.L., Greenop R., Foster G.L., Lear C.H. (2020) Ocean Carbon Storage across the Middle Miocene: A new interpretation for the Monterey Event. *Nature Communications*. 11, 134. DOI:https://doi.org/10.1038/s41467-019-13792-0

Strand K. (2005) Sequence stratigraphy of the siliciclastic east Puolanka Group, the Palaeoproterozoic Kainuu Belt, Finland. *Sedimentary Geology*, V. 176, p. 149–166. DOI:http://dx.doi.org/10.1016/j.sedgeo.2004.12.014

Stow D., Nicholson U., Kearsey S. (2020) The Pliocene-Recent Euphrates River system: sediment facies and architecture as an analogue for subsurface reservoirs, *Energy Geoscience* 1 (3–4)174–193. DOI:https://doi.org/10.1016/j.engeos.2020.07.005

Sun J., Sheykh M., Ahmadi N., Cao M., Zhang Z., Tian S., Sha J., Jian Z., Windley B., Talebian M. (2021) Permanent closure of the Tethyan Seaway in the northwestern Iranian Plateau driven by cyclic sea-level fluctuations in the late Middle Miocene. *Palaeogeography, Palaeoclimatology, Palaeoecology* 564 (2021) 110172. DOI:https://doi.org/10.1016/j.palaeo.2020.110172

Teisseyre A.K. (1975) Pebble fabric in braided stream deposits with examples from recent and frozen Carboniferous channels (Intrasudetic Basin, Central Sudetes). *Geology Sdetica* X (1), 7-47.

Teng Z., Peng Z., Xingjian W., Rong Q., Faqi H., Tong M. (2024) Characteristics and model of meandering-river-delta reservoir architecture of member Chang-6 in Fuxian area, Triassic Ordos Basin. *Unconventional Resources*. 4, 100084. DOI:https://doi.org/10.1016/j.uncres.2024.100084

Terquem O. (1875) Essai sur le classement des animaux qui vivent sur le plage et dans les environs de Dunkerque (premier fascicule). *Paris*. DOI: https://gallica.bnf.fr/ark:/12148/bpt6k5614755b/f461

Therrien F. (2006). Depositional environments and fluvial system changes in the dinosaur-bearing Sanpetru Formation (Late Cretaceous, Romania): Postorogenic sedimentation in an active extensional basin. *Sedimentary Geology*, V. 192, p. 183–205. DOI:https://doi.org/10.1016/j.sedgeo.2006.04.002

Torfstein A., Steinberg J. (2020) The Oligo–Miocene closure of the Tethys Ocean and evolution of the proto-Mediterranean Sea. *Science Reviews*. 10, 13817. DOI:https://doi.org/ 10.1038/s41598-020-70652-4

Tucker M.B. (2003) Sedimentary Rocks in the Field. 3rd ed., *John Wiley & Sons*, 234 p. DOI:https://10.2113/gseegeosci.18.4.401-b

Tucker M.E. (2001) Sedimentary Petrology: Third Edition, *Blackwell, Oxford*, p. 260. DOI:https://doi.org/10.1017/S0016756802266510

Tucker M.E. (1991) Sedimentary Petrology: An introduction to the origin of sedimentary rocks. *Blackwell Scientific Publication*s, 260 p

Vandenberghe J., Kasse K., Gábris G.Y., Bohncke S., Van Huissteden K. (2003) Fluvial style changes during the last 35.000 years in the Tisza valley. *International Quaternary Research Union*, 23–30 July 2003, Reno, Nevada, USA, Abstracts, p. 68. DOI:https://10.1016/j.pgeola.2010.02.005

Vergès J., Emami H., Garcés M., Beamud E., Homke S., Skott P. (2019) Zagros foreland fold belt timing across Lurestan to constrain Arabia–Iran collision. In: Saein, A. (Ed.), Tectonic and Structural Framework of the Zagros Fold-Thrust Belt. *Elsevier*, pp. 29–52. DOI:https://doi.org/10.1016/B978-0-12-815048-1.00003-2

Williams P.F., Rust B.R. (1969) The sedimentology of a braided river. *Journal of Sedimentary Petrology*, 39, 649-679. DOI:https://doi.org/10.1306/74d71cf3-2b21-11d7-8648000102c1865d

Woo J., Shinn Y.J., Kwon Y.K., Chough S.K. (2006) The Janson and Myeonsan formation (Early Cambrian) of the Taebaek Group, Mideast Korea: depositional processes and environments. *Geosciences Journal*, Vol. 10, No. 1,p.35-57. DOI:https://doi.org/10.1007/BF02910331

Yagishita K. (1997) Paleocurrent and analyses of fluvial conglomerates of the Paleogene Noda Group, northeast Japan. *Sedimentary Geology*, 109, 53-71. DOI:https://doi.org/10.1016/S0037-0738(96)00058-9

Zamaniyan E., Khanehbad M., MoussaviHarami R., Mahboubi A. (2018) Lithofacies and sedimentary environment of Qadir Member of the Nayband Formation on Parvadeh Coal Mines region, east-central Iran: *Scientific Quarterly Journal, Geosciences*, 28 (109): 295-304. (in Persian). DOI:https://doi.org/10.22071/gsj.2017.91282.1184

Zamaniyan E., Khanehbad M., Moussavi-Harami R., Mahboubi A. (2021) Sedimentary environment and provenance of sandstones from the Qadir member in the Nayband Formation, Tabas block, east-central Iran. *Boletín de la Sociedad Geológica Mexicana*, 73 (1): A140920, 1-35. DOI:https://doi.org/10.18268/BSGM2020v73n1a140920

Zand-Moghadam H., Moussavi-Harami R., Mahboubi A. (2014) Sequence stratigraphy of the Early–Middle Devonian succession (Padeha Formation) in Tabas Block, East-Central Iran: Implications for mixed tidal flat deposits. *Palaeoworld*, V. 23, p. 31-49. DOI:https://doi.org/10.1016/j.palwor.2013.06.002